

University of Alberta

The Recession of Bitumen from a Silica Surface under Shear Flow

by

Justin Robert Walker ©

A thesis submitted to the Faculty of Graduate Studies and Research
in partial fulfillment of the requirements for the degree of

Master of Science
in
Chemical Engineering

Department of Chemical and Materials Engineering

Edmonton, Alberta
Fall, 2006



Library and
Archives Canada

Bibliothèque et
Archives Canada

Published Heritage
Branch

Direction du
Patrimoine de l'édition

395 Wellington Street
Ottawa ON K1A 0N4
Canada

395, rue Wellington
Ottawa ON K1A 0N4
Canada

Your file *Votre référence*
ISBN: 978-0-494-22400-7
Our file *Notre référence*
ISBN: 978-0-494-22400-7

NOTICE:

The author has granted a non-exclusive license allowing Library and Archives Canada to reproduce, publish, archive, preserve, conserve, communicate to the public by telecommunication or on the Internet, loan, distribute and sell theses worldwide, for commercial or non-commercial purposes, in microform, paper, electronic and/or any other formats.

The author retains copyright ownership and moral rights in this thesis. Neither the thesis nor substantial extracts from it may be printed or otherwise reproduced without the author's permission.

AVIS:

L'auteur a accordé une licence non exclusive permettant à la Bibliothèque et Archives Canada de reproduire, publier, archiver, sauvegarder, conserver, transmettre au public par télécommunication ou par l'Internet, prêter, distribuer et vendre des thèses partout dans le monde, à des fins commerciales ou autres, sur support microforme, papier, électronique et/ou autres formats.

L'auteur conserve la propriété du droit d'auteur et des droits moraux qui protègent cette thèse. Ni la thèse ni des extraits substantiels de celle-ci ne doivent être imprimés ou autrement reproduits sans son autorisation.

In compliance with the Canadian Privacy Act some supporting forms may have been removed from this thesis.

Conformément à la loi canadienne sur la protection de la vie privée, quelques formulaires secondaires ont été enlevés de cette thèse.

While these forms may be included in the document page count, their removal does not represent any loss of content from the thesis.

Bien que ces formulaires aient inclus dans la pagination, il n'y aura aucun contenu manquant.


Canada

Abstract

The recession of bitumen from a silica surface under shear flow has been studied in both couette flow between rotating cylinders, and channel flow between flat plates. The effect of temperature, shear, and water chemistry on the recession rate of bitumen from a silica surface is studied by subjecting a bitumen coated silica plate to shear flow under varying conditions and analysing the rate at which the bitumen is removed from the surface.

Increasing temperature and shear rate were found to accelerate bitumen recession.

Increasing divalent ion concentration was found to impair bitumen recession. Changes in the composition of industrial process water were not found to significantly alter bitumen recession. Furthermore, elevated temperatures were found to have an irreversible effect on the chemistry of industrial process water. The bitumen recession device developed in this study is a novel tool for analysing the effect of process variables on oil sands extraction.

Acknowledgements

I would like to thank my supervisors, Dr. Jacob Masliyah and Dr. Zhenghe Xu, for their guidance and assistance over the last two years. It has been a wonderful experience working for these two brilliant professors. I would like to thank Dr. Jaewon Choung for helping me get started in the field, and for all his assistance in the preliminary and theoretical portions of this project.

I would also like to thank the members of the Oil Sands research group, in particular Jim Skwarok for his invaluable help in the lab, Aref Seyyed Najafi for his mathematical insights, and Hongying Zhao for help with the process water froth fractionation apparatus. I would also like to thank the skilled craftsmen in the machine shop and the glass shop for making my crude sketches a reality.

Thanks go to my family and friends; and in particular to my wife Lindsay for supporting me. I may not have finished before the wedding like I promised, but she stuck by me anyway.

Lastly, I would like to thank the NSERC Chair program in Oil Sands Extraction and its sponsors for financial support.

This thesis is dedicated to my wife Lindsay, and my family; Don, Shirley, Matthew,
Kristin, Gail, Michael, Laelie and Lisa.

Table of Contents

Chapter 1	Introduction	1
1.1	Introduction to thesis	1
1.2	Background information	2
1.3	Bitumen recession	4
1.4	Interfacial forces responsible for recession	5
1.5	Previous works	7
Chapter 2	Recession of bitumen from a glass surface in a co-axial cylinder device	11
2.1	Introduction to chapter two	11
2.2	Experimental procedure	17
2.2.1	Slide preparation	17
2.2.2	Bitumen preparation	18
2.2.3	Slide coating	18
2.2.4	Solution preparation	18
2.2.5	Experimental	19
2.2.6	Data analysis	19
2.3	Results and discussion	20
2.3.1	Effect of temperature	20
2.3.2	Effect of divalent ions	25
2.3.3	Effect of pH	28
2.3.4	Industrial recycle process water	30
2.3.5	Overall results	32

2.4	Conclusions and recommendations	32
Chapter 3	Recession of bitumen from a quartz surface in a channel flow device	34
3.1	Introduction to chapter three	34
3.2	Experimental procedure	37
	3.2.1 Experimental preparation	37
	3.2.2 Process water foam fraction preparation	37
	3.2.3 Experimental	39
3.3	Results and discussion	40
	3.3.1 Test for reproducibility	40
	3.3.2 Effect of temperature	42
	3.3.3 Effect of shear	43
	3.3.4 Effect of process water composition	45
	3.3.4.1 Effect of process water foam fractions	46
	3.3.4.2 Effect of process water source	48
	3.3.4.3 Effect of surfactant co-precipitation with calcium carbonate	50
	3.3.5 Oil sand ore	51
	3.3.6 Overall results	54
3.4	Conclusions	54
Chapter 4	Effect of temperature on the stability of froth formed in the recycle process water of oil sands extraction	56
4.1	Introduction to chapter four	56
4.2	Experimental	59
	4.2.1 Materials and apparatus	59

4.2.2	Experimental procedures	60
4.2.3	Experimental results	61
4.3	Discussion	64
4.4	Conclusions	70
Chapter 5	Summary and recommendations	72
	Bibliography	75

List of Tables

Table 2.1:	Simulated process water components	31
Table 3.1:	Reynolds numbers for various flowrates	44
Table 3.2:	Water chemistry of industrial process water samples	50
Table 4.1:	Properties of the recycle process water used for testing	59

List of Figures

Figure 1.1:	Visual representation of the process of bitumen liberation	5
Figure 1.2:	Effect of temperature on the change in contact angle over time for a bitumen droplet on a glass surface	8
Figure 1.3:	Effect of pH on the change in contact angle over time for a bitumen droplet on a glass surface	9
Figure 2.1a:	Schematic overview of the co-axial cylinder device	12
Figure 2.1b:	Schematic overview of the co-axial cylinder device – side view	12
Figure 2.1c:	Schematic diagram of outer glass cylinder component	13
Figure 2.1d:	Schematic diagram of inner stainless steel cylinder component	14
Figure 2.1e:	Schematic diagram of slide holding bracket component	15
Figure 2.2:	Photograph of co-axial cylinder device	16
Figure 2.3:	Typical recession curves for experiments at different temperatures	20
Figure 2.4:	Effect of temperature on bitumen recession	21
Figure 2.5:	Bitumen viscosity variation with temperature	22
Figure 2.6:	Change in recession time with bitumen viscosity	23
Figure 2.7:	Estimation of surfactant migration time at different temperatures	24
Figure 2.8:	The effect of calcium ion concentration on bitumen recession	26
Figure 2.9:	Zeta potential distribution of the bitumen-silica system in the presence of 1 mM calcium ions	27
Figure 2.10:	Comparison of Calcium and Magnesium Ions	28
Figure 2.11:	Effect of pH on bitumen recession rate in a deionized water system	29
Figure 2.12:	Effect of temperature on recession in industrial process water	30

Figure 2.13:	Comparison of the process water system with the deionized water system	32
Figure 3.1a:	Schematic overview of channel flow apparatus	34
Figure 3.1b:	Schematic diagram of channel flow cell	35
Figure 3.2:	Photographic close-up of flow cell	36
Figure 3.3:	Schematic illustration of frothing column	38
Figure 3.4:	Time to 50% recession for 12 individual slides	41
Figure 3.5:	Effect of temperature on bitumen recession	43
Figure 3.6:	Effect of shear stress on recession rate	45
Figure 3.7:	Recession of bitumen in process water foam fractions	46
Figure 3.8:	Recession curves for process water foam fractions	47
Figure 3.9:	Recession rate for differently sourced process waters	49
Figure 3.10:	Effect of surfactant depletion by co-precipitation on bitumen recession	51
Figure 3.11:	Modified sample cell for oil sands ore	52
Figure 3.12:	Recession of bitumen from oil sand ore – observed <i>in situ</i>	53
Figure 4.1:	Schematic illustration of experimental set-up	60
Figure 4.2:	Effect of recycle process water temperature on the froth height	62
Figure 4.3:	Size distributions of bubbles generated using two different Spargers	62
Figure 4.4:	Typical images of bubbles generated using (a) a fine and (b) a coarse sparger at 30°C; one small division = 1 mm	63
Figure 4.5:	Effect of recycle process water temperature on the froth height as a function of superficial air velocity	64
Figure 4.6:	Effect of recycle process water temperature on the froth height and the bubble size distribution	65

Figure 4.7:	Effect of precipitate on the froth height	66
Figure 4.8:	EDX results obtained with the precipitate formed in recycle process water at 70°C	68
Figure 4.9:	XRD results obtained with the precipitate formed in recycle process water at 70°C	69
Figure 4.10:	FTIR results obtained with the precipitate formed in recycle process water at 70°C	70

List of Abbreviations and Symbols:

κ	Ratio of inner cylinder radius to outer cylinder radius
σ_{bw}	Bitumen-water interfacial tension
σ_{bs}	Bitumen-silica interfacial tension
σ_{sw}	Silica-water interfacial tension
σ_{surf}	Surface energy
θ_e	Equilibrium contact angle
Ω_i	Angular velocity of inner cylinder
ρ	Fluid density
τ_w	Shear stress at the wall
$\tau_{r\theta}$	Shear stress in direction θ at radius r
μ_f	Fluid viscosity
ν	Kinematic viscosity
v_x	Contact line velocity
CCD	Charge Coupled Device
CHWE	Clark Hot Water Extraction Process
cm	centimetres
DRIFTS	Diffuse Reflective Infrared Fourier-Transform Spectroscopy
EDX	Energy Dispersive X-ray spectroscopy
FTIR	Fourier Transform Infrared Spectrometer
G	Acceleration due to gravity – 9.81 m/s ²
g	gram

k	dimensionless constant
MIBC	Methyl iso-butyl carbinol (a frothing agent)
m	metres
mM	millimoles per litre
mN	millinewtons
mV	millivolts
PTFE	Polytetraflouroethylene
r	Radius
R_i	Radius of inner cylinder
R_o	Radius of outer cylinder
Re	Reynolds number
s	seconds
Ta	Taylor number
u_θ	velocity in the angular direction
U_i	Peripheral velocity of inner cylinder
U_∞	Fluid velocity away from the wall
$\langle x^2 \rangle$	Mean squared displacement
XRD	X-ray Diffraction spectroscopy

Chapter 1 - Introduction

1.1 Introduction to thesis

The recession of bitumen from a silica surface is of critical importance to the oil sands extraction process, as it is the first step in the recovery of bitumen from the oil sands. An oil sands ore consists primarily of quartz sand grains. The voids between sand grains are filled with bitumen, fine clay particles, salts, and connate water. Athabasca bitumen is an extremely viscous, complex hydrocarbon mixture containing varying levels of metal ions and water-soluble surfactants (Moschopedis and Speight, 1971; Ali, 1978; Schramm and Smith, 1987), and is chemically similar to a heavy conventional crude oil.

In order for bitumen to be recovered from the oil sands, the bitumen must be disengaged, or simply liberated from the sand grains. This is achieved by exposing the ore to water. Since the sand grains are generally hydrophilic, the bitumen film is displaced by water and recedes to form droplets. These droplets are then able to transfer from the sand grain to the slurry and attach to air bubbles. The aerated bitumen can be separated from the sand grains on the basis of their buoyancy.

It is the aim of the industry to develop a process by which the bitumen recedes as quickly as possible. This allows for a maximization of the throughput of the plant, and a minimization of the amount of ore that needs to be retained in the system, allowing for smaller equipment, and a more efficient process. A detailed understanding of the effect of process variables on bitumen recession is required for the development or optimization of such a process.

Previous studies in the field have concerned themselves with the recession of bitumen from model surfaces – glass and mica – in the absence of shear. The current study represents the first in the oil sands extraction field to investigate the recession of bitumen under shear flow. This is necessary, as during the oil sands extraction process, the bitumen-laden sand grains are subjected to significant shear forces – especially as the

slurry passes through a pump. While the primary separation vessel is relatively quiescent, the majority of bitumen should be fully liberated before entering the vessel in order to be recovered, and as such the study of bitumen recession under shear is extremely important to the development of our understanding of the oil sands extraction process.

The purpose of this study is to investigate the effect of process variables; such as temperature, pH, and electrolyte composition; on the recession rate of bitumen from a silica surface. We are also interested in the comparison of the laboratory- prepared aqueous solutions (hereinafter referred to as ‘model’ solutions) used in the past with industrial recycle process water, and the effect of the process variables on that water itself.

The first chapter of this thesis will introduce the reader to the oil sands extraction process, the concept of recession and the physics behind it, and briefly discuss the previous studies in this field. The second chapter will look at the effect of temperature, pH, and divalent ion concentration on the recession rate of bitumen from a glass slide in a co-axial cylinder device; using model solutions as well as industrial recycle process water. The third chapter will look at the effect of temperature, industrial water composition, shear stress, and bicarbonates on the recession rate of bitumen from a quartz surface in a channel flow apparatus. Chapter 4, a paper previously published in the *Canadian Journal of Chemical Engineering*, investigates the effect of process water treatment on its composition, and how that relates to oil sands extraction. Chapter 5 contains the summary and conclusions of the work.

1.2 Background information

Extraction of bitumen from the Athabasca oil sands in northern Alberta represents one of the world’s single largest energy reserve. Conservative estimates of the reserve predict that some 175 billion barrels of synthetic crude oil are recoverable from the oil sands using current technology, making it the second largest single oil reserve in the world next

to Saudi Arabia (Radler, 2002). Industry insiders estimate that in excess of 2 trillion barrels of synthetic crude are in place in the oil sands deposit, and that the development of new technologies will allow these additional resources to be exploited. The development of these technologies will rely heavily on the fundamental understanding of the behaviour of oils sands extraction systems. Current production is around 1 million barrels per day, and the industry estimates that by 2030, production from the oil sands will reach some 5 million barrels per day from a combination of surface mining and in situ production techniques (Resources, 2004). Currently, bitumen extracted from the Athabasca oil sands accounts for at least 25 % of total oil production in Canada, a number which is steadily increasing as conventional oil reserves in Canada dwindle, and as new oil sands production is brought on line.

Synchrude Canada Ltd., Suncor Energy Inc., and more recently Albian Sands Inc., and Canadian Natural Resources have successfully implemented commercial exploitation of the Athabasca oil sands using a modified version of the Clark Hot Water Extraction (CHWE) process (Baptista and Bowman, 1969; Hepler and Smith, 1994). This process involves mixing oil sands ore with warm water in a hydrotransport pipeline, in which bitumen ablation and liberation from sand grains take place. First, the oil sand is crushed into manageably sized lumps and is digested in warm water. The conventional CHWE process operates at temperatures approaching 75°C in order to lower the viscosity of bitumen to facilitate bitumen liberation and handling. This process is energy-intensive due to the necessity of heating large quantities of water to such high temperatures. Consequently, the oil sands industries have been focussing on the development of lower-energy extraction alternatives where the lower thermal energy is made up through the addition of process aids such as kerosene and/or MIBC. In either process, natural surfactants present in the oil sands assist in lowering the interfacial tension between bitumen and the aqueous phase of the oil sands slurry. This leads to the formation of a three phase bitumen-water-solid contact line, from which the bitumen recedes to form a drop and eventually detaches from the sand grains. This is the critical first step in the process of recovering bitumen from oil sands for eventual production of synthetic crude oil. Once detached from the sand grains, the bitumen droplets are free to attach to air

bubbles entrained or introduced into the slurry. Aerated bitumen droplets float to the top of the slurry to form a bitumen-rich froth in a primary gravity separation vessel.

The bitumen froth is then deaerated and sent to a “froth treatment” plant, where the froth is diluted with a solvent – commonly naphtha – and water and entrained solids are removed through a combination of inclined plate settling and centrifugation techniques. Any bitumen droplets remaining in the slurry are further recovered using conventional mechanical or column flotation cells before being sent to froth treatment. The clean, dry froth product is then sent for solvent recovery and upgrading to produce a synthetic crude oil product which is sold to oil refineries for the production of a variety of products such as gasoline, diesel fuel, and specialty chemical feed stocks (Syn crude Canada, 2006).

1.3 Bitumen recession

The term recession is defined for the purposes of this thesis as a combination of the ablation and detachment steps of the liberation process – the steps in which a bitumen film ruptures and recedes to form droplets, and then is detached from the solid surface by shear. Figure 1.1 illustrates the process graphically. As with any interfacial phenomena, the recession of bitumen from a silica surface is influenced by many factors including, but not limited to, bitumen viscosity (a strong function of temperature) (Jacobs, Donnelly et al., 1980), pH and electrolyte concentration. It has been well documented in literature that oil sands extraction processes are more effective at higher temperature (Schramm, Stasiuk et al., 2003), and that the presence of calcium and magnesium ions depressed bitumen recovery (Masliyah, Zhou et al., 2004). It has also been shown that a pH of 8.5-10.5 is favourable for oil sands extraction, although this may be primarily due to the role of NaOH's in surfactant production and Ca^{2+} precipitation. While it is understood that temperature, pH and divalent cations affect the overall bitumen recovery process, it is not well understood how they affect the individual steps in the recovery process – the recession of bitumen from silica, the detachment of bitumen droplets from the sand grains, the attachment and engulfment of air bubbles by bitumen droplets and the rise and recovery of air-bitumen aggregates.

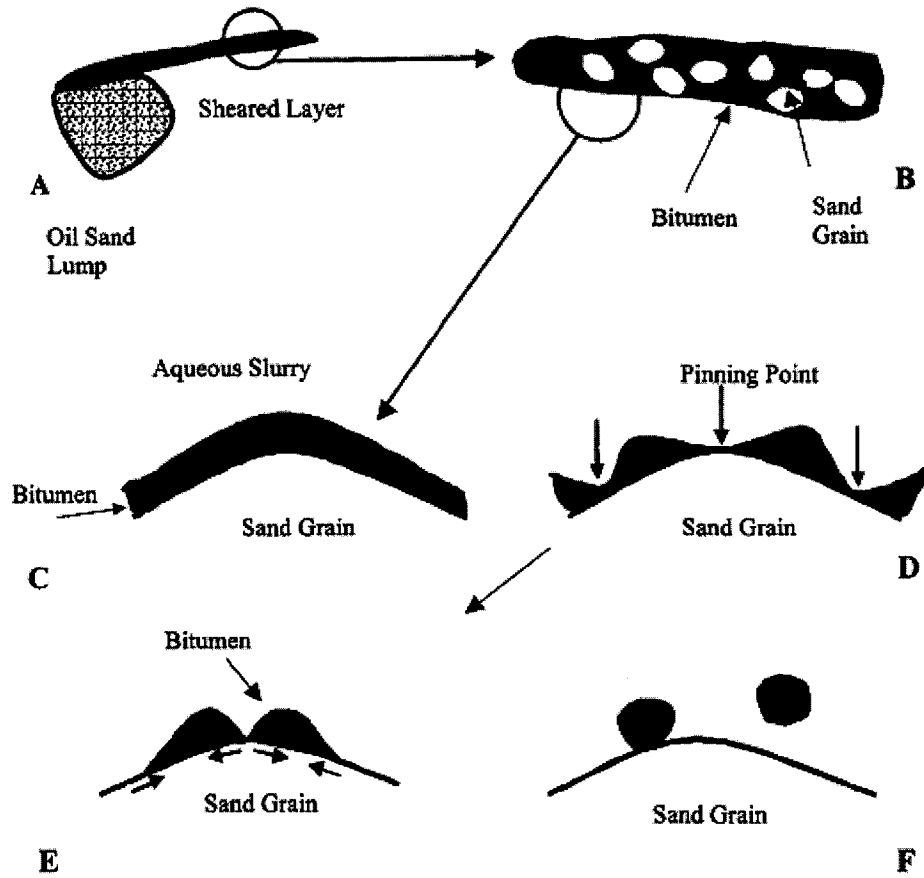


Figure 1.1: Visual representation of the process of bitumen liberation (Adapted from Wallwork, Xu et al., 2004)

1.4 Interfacial forces responsible for bitumen recession

Bitumen recession is governed by the balance of interfacial forces between the three phases present. The interfacial tensions between bitumen-water, bitumen-silica, and water-silica need be considered (Basu, Nandakumar et al., 1996). The Young–Dupré equation (Equation 1.1) illustrates the relation of these parameters with the equilibrium contact angle.

$$\sigma_{ws} = \sigma_{bs} - \sigma_{bw} \cos \theta_e \quad (1.1)$$

where σ_{ws} is water/solid interfacial tension, σ_{bw} is bitumen/water interfacial tension, σ_{bs} is bitumen/solid interfacial tension, and θ_e is the equilibrium contact angle. An equilibrium contact angle of 180° corresponds to the formation of a perfectly spherical droplet, which is only tangentially attached to the solid substrate. This is our ideal case for recession, as in this case the droplets may be easily sheared from the solid surface. Equation 1.1 is useful for determining if a bitumen-water-silica system will recede, but is not useful for determining the rate at which recession is to occur. The effect of bitumen viscosity can be significant at low temperature, but viscosity, being a dynamic property, is not included in this equation.

To that end, Equation 1.2 (Redon, Brochard-Wyart et al., 1991) relates the contact line recession velocity to the equilibrium contact angle, fluid viscosity and surface energy of the liquid.

$$v_x = k\sigma_{surf} \left(\frac{\theta_e^3}{\mu_f} \right) \quad (1.2)$$

where v is the contact line recession velocity, σ_{surf} is the surface energy, k is a constant, and μ_f is the liquid (e.g. oil) viscosity.

Substituting equation 1.1 into equation 1.2, we can derive an expression for the contact line velocity that is independent of contact angle – useful for experiments where the recession is observed from an angle where the contact angle cannot be observed.

$$v_x = k\mu_f^{-1}\sigma_{surf} \left[\cos^{-1} \left(\frac{\sigma_{bs} - \sigma_{ws}}{\sigma_{bw}} \right) \right]^3 \quad (1.3)$$

Equation 1.3 implies that the surface velocity is constant for a particular set of interfacial tensions, viscosities, and surface energies. This is found to be the case in many systems (Shull and Karis, 1994). However, Basu, Nandakumar et al., 1996 found that this is not the case in the bitumen-glass-water system. They observed that the contact line velocity is fastest at the initial rupture of the film, and then gradually decreases. Other models (Foister, 1990; Cox, 1986) fare better in predicting contact line velocities with varying

viscosity, but some uncertainty remains. It is evident that there is no reliable model for the accurate prediction of contact line velocity – and therefore recession rate. It is the author's hope that the data presented in this work will be helpful in the development of such a model.

1.5 Previous works

A number of studies concerning the interfacial interactions of the bitumen-water-silica system have been performed in the past. Basu, Nandakumar et al., 1996 investigated the static (no shear) displacement of bitumen from microscope glass (hydrophilic) and PTFE (hydrophobic) surfaces. They found that the equilibrium contact angle and recession rate of a bitumen droplet on a glass surface were dependant on pH and temperature. Figure 1.2, adapted from that work, clearly shows the change in the recession rate at different temperatures. They also showed the clear effect of pH on the bitumen recession process. As seen in Figure 1.3, the equilibrium contact angle at an acidic pH is much lower than at higher pH, but the recession occurs faster. They also observed that little to no recession occurs on a hydrophobic surface, as the bitumen- PTFE equilibrium contact angle in water is near 180° as measured through water (complete spreading).

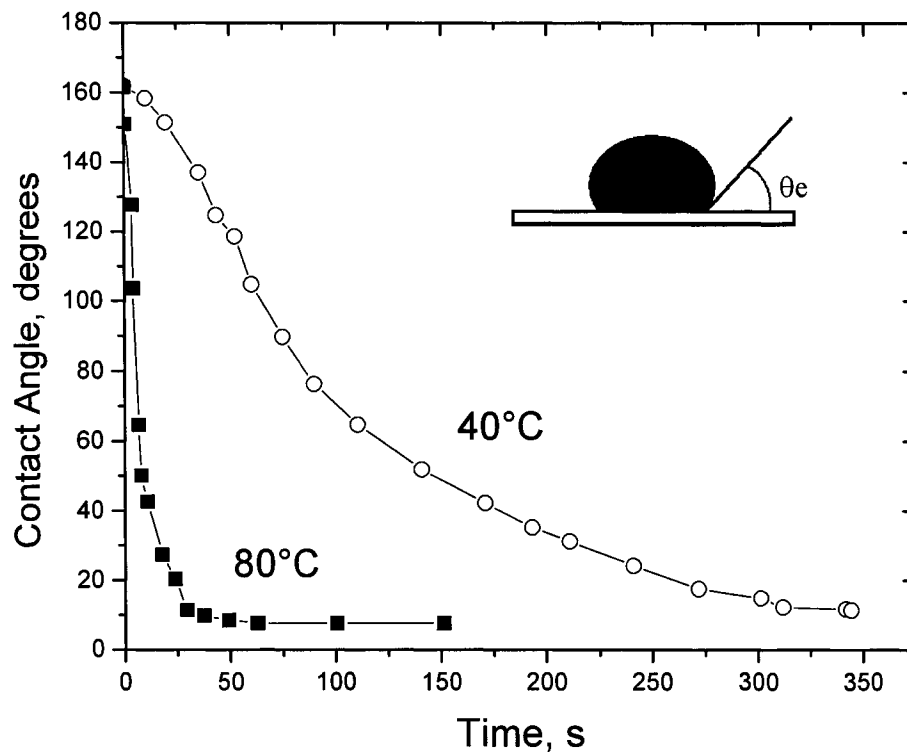


Figure 1.2 - Effect of temperature on the change in contact angle over time for a bitumen droplet on a glass surface (Adapted from Basu, Nandakumar et al., 1996)

The effect of calcium ions on bitumen recession was investigated in a later study (Basu, Nandakumar et al., 2004). In this study, it was found that both time variation of bitumen dynamic contact angle and bitumen equilibrium contact angle were affected by the presence of calcium ions during bitumen droplet recession. In their study, synergistic effects of montmorillonite clays with the calcium ions were not observed. However, individually, calcium ions and montmorillonite clays were able to suppress the recession rate and equilibrium contact angle in the bitumen-deionized water-glass system. Their study showed that when varying the calcium ion concentration from 0 ppm to 100 ppm, the equilibrium contact angle (measured through bitumen) decreased from approximately 170° to 130°, and the time to reach equilibrium increased by roughly an order of magnitude.

Another interesting result from the work of Basu, Nandakumar et al., 2000 was the formation of “daughter droplets” during the recession of bitumen from a glass surface.

This study showed that when the initial bitumen film deviated from the perfect circular film used in their previous studies, the film receded unevenly and ruptured to form a series of smaller droplets, rather than one single droplet. They also found that the size and quantity of these droplets was dependant on the geometry of the bitumen film and, to a lesser degree, on the solution pH. Therefore, one would expect in an experiment with a non-circular geometry – such as in this study – that recession will not be uniform, and a bitumen film will rupture to form several droplets, rather than a single droplet.

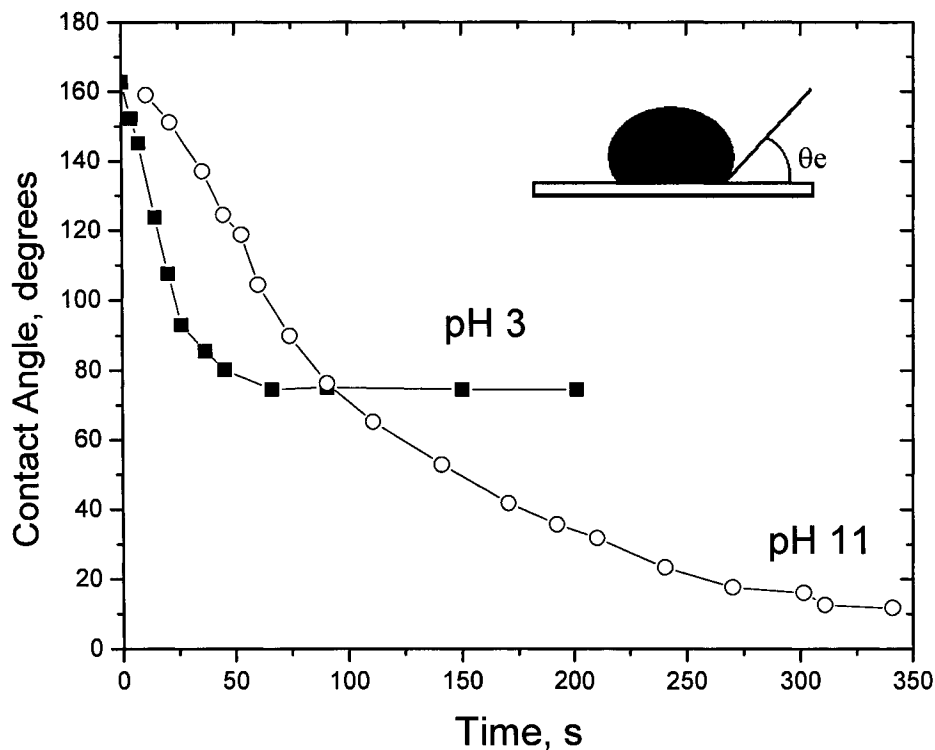


Figure 1.3 - Effect of pH on the change in contact angle over time for a bitumen droplet on a glass surface (Adapted from Basu, Nandakumar et al., 1996)

Numerous studies have been performed to study and model the wetting of thin liquid films on solid substrates, but very few have looked at the reverse process. Redon, Brochard-Wyart et al., 1991 studied the dynamics of dewetting for a thin, metastable film of silicone on a silicon substrate, and developed a number of semi-empirical equations to predict the rate of dewetting for the system. The bitumen-silica system can be considered

to be metastable in (the presence of) air, but becomes unstable once exposed to water due to the change in the bitumen-water and bitumen-air interfacial tensions.

Basu and Sharma, 1996 studied a model system of a model oil (hexadecane) on glass and mica surfaces. While the study was primarily concerned with using atomic force microscopy to determine disjoining pressure isotherms, it introduced the concept of using a bitumen film coated on a silica surface as a tool for oil sands extraction research.

The study of bitumen recession from sand grains was also studied (Basu, Nandakumar et al., 1998). In this study, a sand grain derived from an oil sands ore was viewed under high magnification, and the film rupture and droplet formation were observed. This process, as with all previous studies in this field, was performed in a shear-free environment. It showed that the recession of bitumen from a sand grain followed the same mechanism as recession from a flat plate, and that the results from the two are comparable.

Chapter 2 – Recession of bitumen from a glass surface in a co-axial cylinder device:

2.1 Introduction to chapter two

This chapter illustrates the effect of temperature, divalent ions, and pH on the recession of bitumen from a glass surface in aqueous solutions in a co-axial cylinder device. The device and its constituent components are illustrated schematically in Figures 2.1a, 2.1b, 2.1c, 2.1d, and 2.1e, and shown photographically in Figure 2.2. The experimental apparatus consists of the coaxial cylinder device, a modified drill press, a CCD camera, and a computer.

Glass slides were used in this experiment as our model surface for a number of reasons. First; glass surfaces have been used in the majority of the previous studies in this field. Therefore, it is advantageous to use a glass surface, so that our results may be contrasted with the results of those in other studies. Secondly; our experimental setup depends on optical transparency of the model surface, as a light transmission technique is used to analyse the quantity of bitumen remaining on the surface. Since bitumen is opaque, any areas where light cannot pass through the slide can be assumed to be bitumen-coated, provided the surface itself is transparent. Thirdly; since the oil sands ore sand grains are largely hydrophilic, it was desirable to choose a water-wet solid as our model surface. Glass microscope slides, especially after exposure to a strong acid, exhibit a contact angle of water-in-air of nearly 180° (measured through air), indicating a strongly hydrophilic surface.

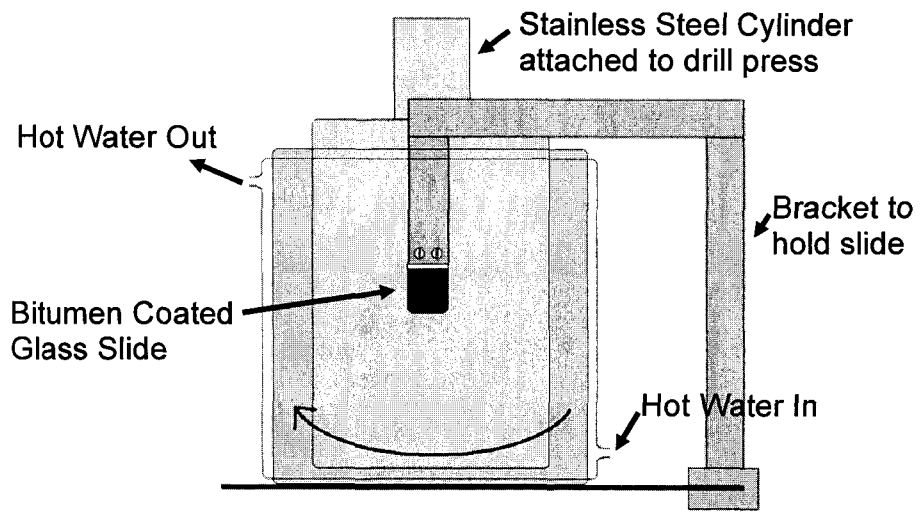


Figure 2.1a – Schematic overview of the co-axial cylinder device.

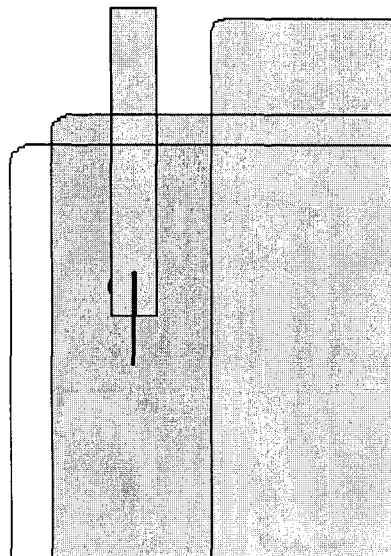


Figure 2.1b – Schematic overview of the co-axial cylinder device – side view.

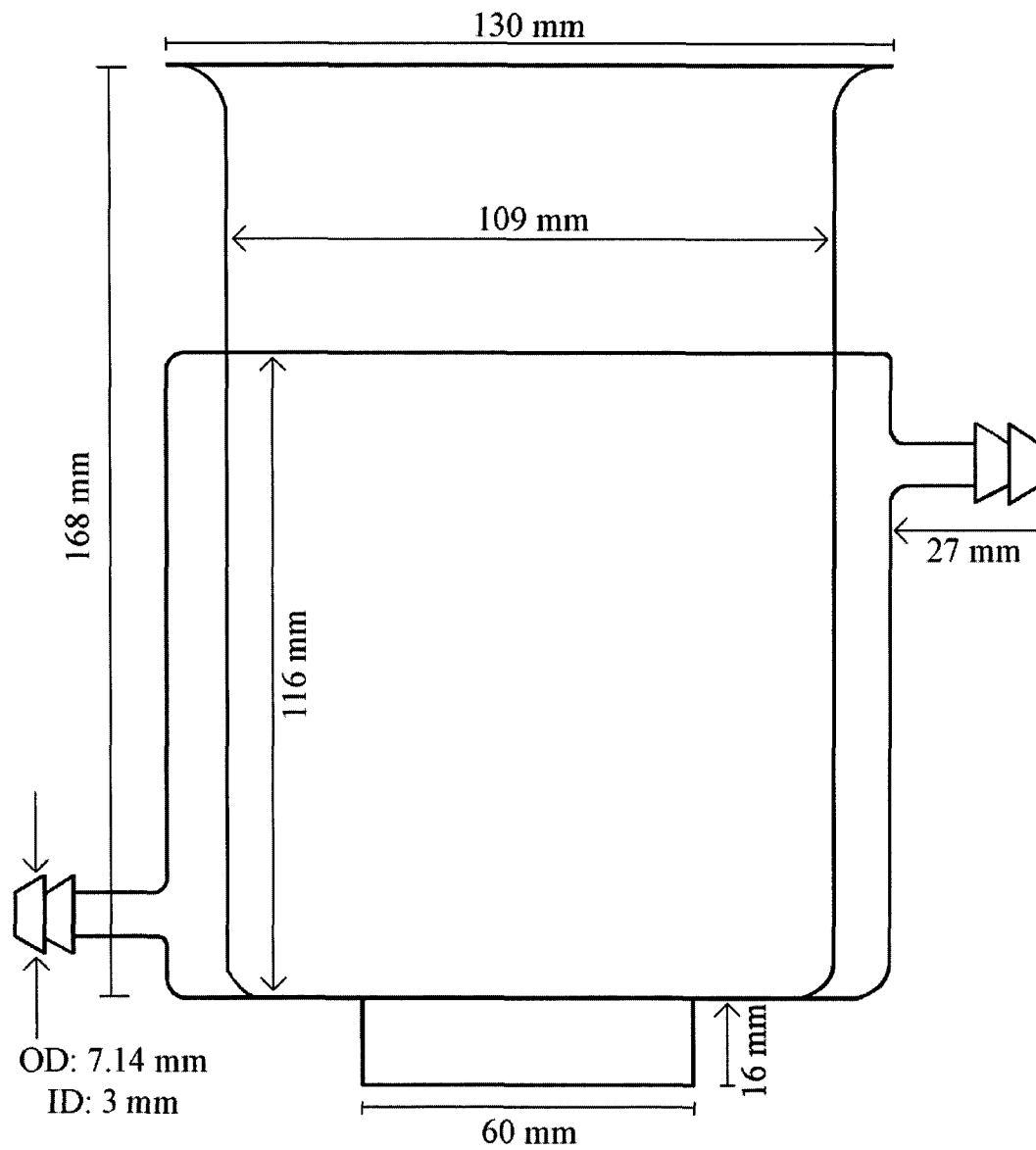


Figure 2.1c – Schematic diagram of outer glass cylinder component

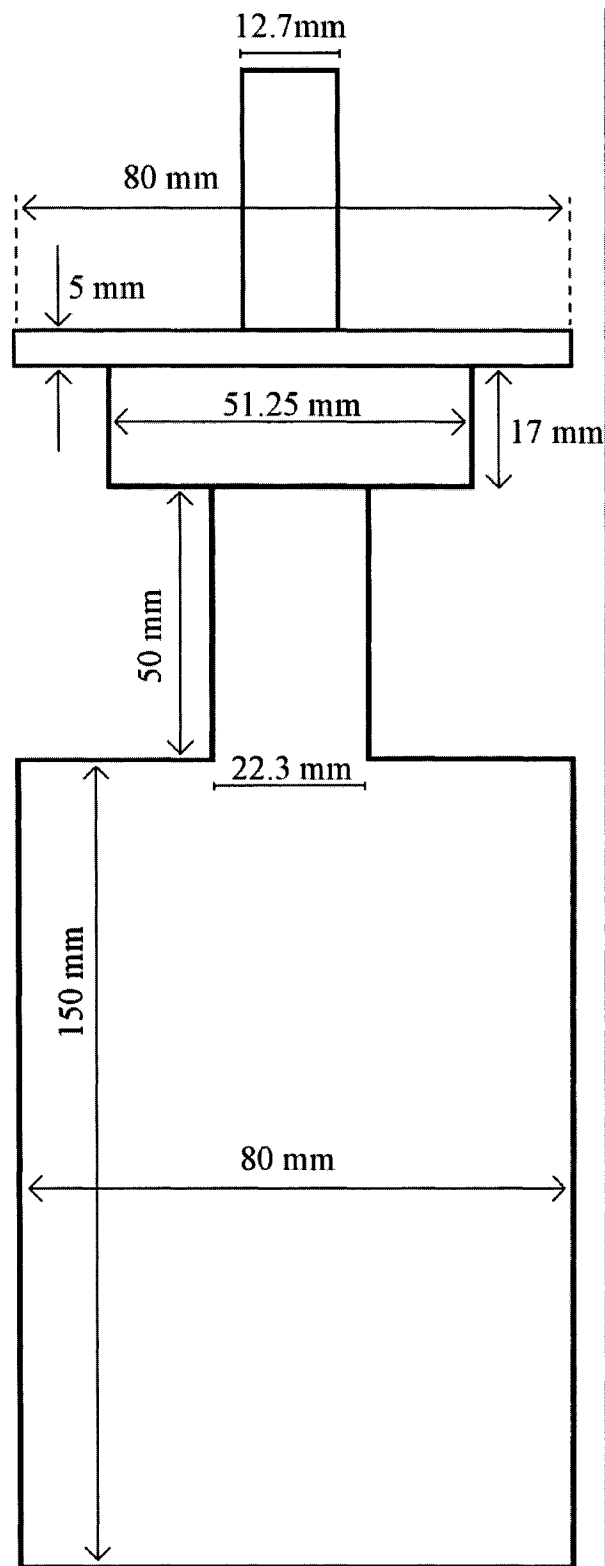


Figure 2.1d – Schematic diagram of inner stainless steel cylinder component (rotor)

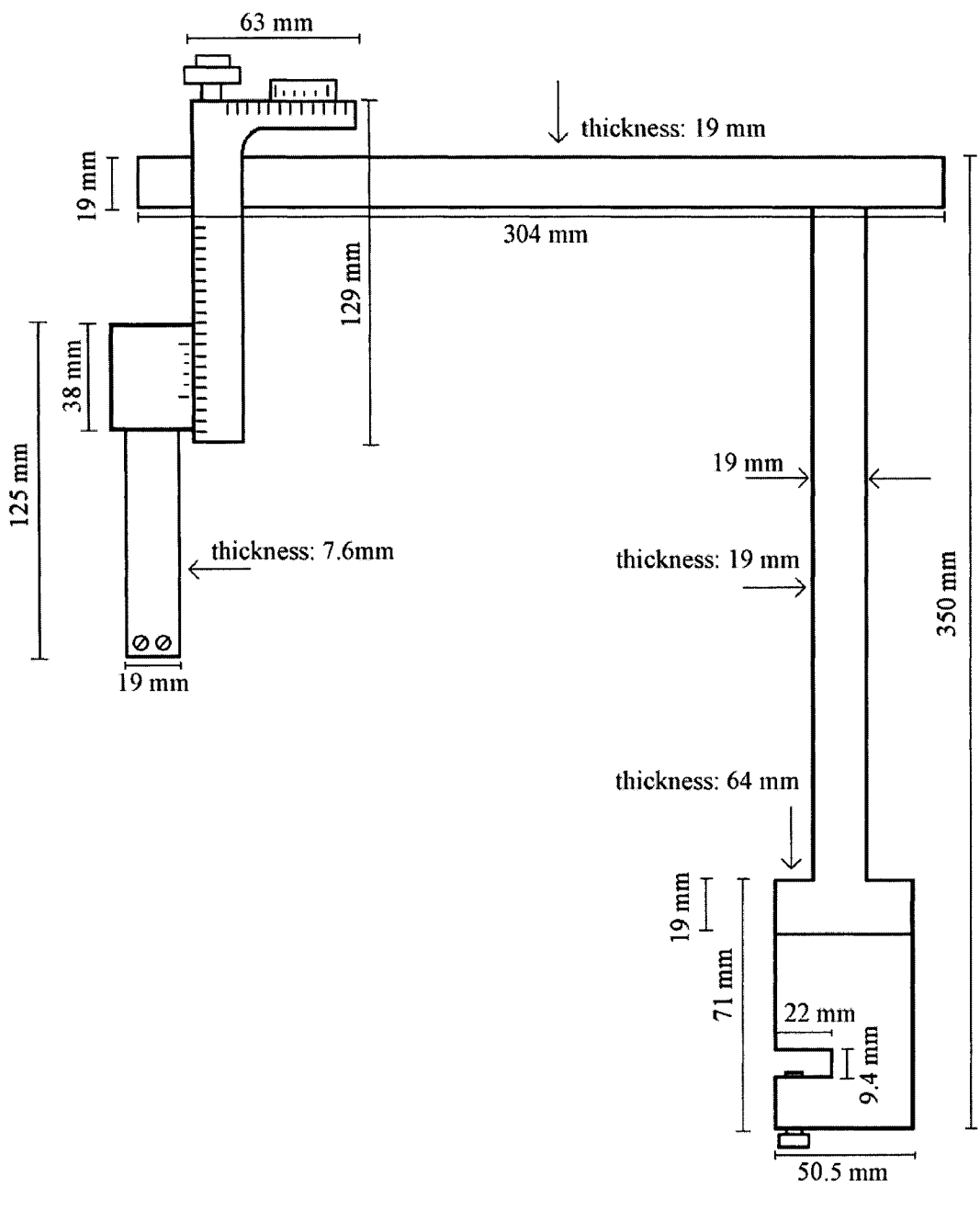


Figure 2.1e – Schematic diagram of slide holding bracket component



Figure 2.2 – Photograph of co-axial cylinder device

As the flow in this experimental apparatus is Couette-type flow, the velocity profile can be described by equation 2.1 (Bird, Stewart et al., 2002).

$$u_{\theta} = \Omega_i \kappa R \frac{\left(\frac{R}{r} - \frac{r}{R} \right)}{\left(\frac{1}{\kappa} - \kappa \right)} \quad (2.1)$$

where u_{θ} is the velocity in the angular direction at radius r , Ω_i is the angular velocity, R is the outer (fixed) cylinder radius, and κ is the ratio of the inner cylinder radius to the outer cylinder radius. The shear stress within the gap is given by:

$$\tau_{r\theta} = -\mu \frac{du_{\theta}}{dr} \quad (2.2)$$

Performing the differentiation of equation 2.1, the result is:

$$\tau_{r\theta} = -\mu \left[\frac{\Omega_i \kappa^2 (r^2 + R^2)}{r^2 (\kappa^2 - 1)} \right] \quad (2.3)$$

Using the geometry of the experimental setup, where $\kappa = 40/54.5$, $r = 47.25$ mm, $R = 54.5$ mm, $\Omega_i = 6.7$ s⁻¹, and $\mu = 0.65$ mPa·s, we calculated the shear stress of the apparatus to be 0.012 Pa. This shear stress is constant throughout all of the tests. It is also desirable to know what flow regime the flow between the two cylinders is, as Couette flow can exhibit Taylor vortices at moderate Taylor numbers while still maintaining laminar flow. Schlichting, 1979 defined the Taylor number in equation 2.4.

$$Ta = \frac{U_i d}{\nu} \sqrt{\frac{d}{R_i}} \quad (2.4)$$

where d (14.0mm) is the gap width, R_i (40 mm) is the inner cylinder radius, U_i (0.267 m/s) is the peripheral velocity of the inner cylinder, and ν (6.56×10^{-7} m²s⁻¹) is the kinematic viscosity of the liquid. Substituting in the appropriate values, we find that the Taylor number is 3500. According to Schlichting, 1979, a Taylor number above 1715 indicates turbulent flow. Therefore, the flow between the two rotating cylinders in these tests is turbulent. Since equation 2.1 is only valid for laminar flow, we must recalculate the shear stress. Garaud and Ogilvie, 2005 proposed a correlation for shear rates in turbulent couette flow. According to their work, for a Reynolds number of 16000, as is the case here, the ratio of the turbulent shear to the laminar shear is approximately 9:1. Therefore, we can conclude that the actual shear stress in this equipment is approximately 0.11 Pa, nine times the value found before using the laminar flow equations.

2.2 Experimental procedure

2.2.1 Slide preparation

Glass Microscope slides are cut into 16mm strips by scoring the glass using a diamond-bit scribe and applying gentle pressure to break apart the glass along the cut. The slides are cleaned by using a hot water and detergent mixture, and are rubbed vigorously by hand to remove fingerprints, dirt, or fine glass shards. The slides are then rinsed

repeatedly in tap water, and again in ultra-pure water (18.2 MΩ cm). The slides are then immersed in 15 N H₂SO₄ for a minimum of 24 hours to render the glass surface hydrophilic. The slides are rinsed twice more with ultra-pure water and dried with a stream of compressed nitrogen gas. A small piece of “magic tape” is folded over one end of the slide, and each slide is placed into a Petri dish fitted with a small filter paper to prevent contamination.

2.2.2 Bitumen preparation

VDU (Vacuum Distillation Unit) feed bitumen is diluted to 2.5% (by mass) in toluene, and shaken until homogenized. The diluted bitumen is centrifuged at 20,000 g for 30 minutes to remove fine solids. The resultant supernatant is then passed through a 0.22 μm filter to further remove solids. The solids free bitumen is evaporated at 40°C under vacuum to remove nearly all the toluene. This product is referred to as “solids free bitumen”, containing approximately 90% bitumen and 10% toluene.

2.2.3 Slide coating

Slides are placed into a Spincoater, which holds the slide onto a rotating chuck with vacuum. Approximately 375 μL of solids free bitumen is placed on top of the stationary slide using a precision pipette. The chuck is then set spinning at 100 RPM for 10s, 2000 RPM for 30s, 5000 RPM for 60s, and 7000 RPM for 600s. This results in a smooth, even coating of bitumen approximately 100 μm thick. The tape is removed after the coating is complete. This results in one end of the slide being free of bitumen to allow for attachment to the experimental setup. The slides are allowed to stand in a dust-free environment for a minimum of 24 hours to ensure any remaining toluene has evaporated.

2.2.4 Solution preparation

For most experiments, deionised water is placed in a beaker on a stirring hotplate, and a magnetic stirrer bar is placed in the beaker. A pH probe and thermometer are used to

measure the temperature and pH of the solution. The desired pH, calcium content, and magnesium content are achieved through appropriate additions of NaOH, HCl, CaCl₂ and MgCl₂. Other experiments were performed using Aurora industrial process water, supplied by Syncrude Canada Ltd. The pH and ion levels of this solution were measured. No chemical modifications were made to the process water.

2.2.5 Experimental

A drill press is used as the drive for the inner cylinder of the co-axial device. In place of a drill bit, a stainless steel cylinder is fitted into the chuck. This cylinder fits inside a glass cylinder, which is fitted with a water jacket for temperature control. A water bath is used to heat or cool the cell to the desired temperature. A stainless steel sample holder arm mounts to the drill press such that a glass slide can be suspended in the middle of the gap between the rotating metal cylinder and the glass cylinder. The pre-prepared solution fills the gap between the metal and glass cylinders. A bright light is used to illuminate the setup. A CCD camera is focused on the surface of the suspended glass slide, and is interfaced with a computer. This computer does not record a video stream, but rather the greyscale intensity of each pixel (a measure of how light or dark the image is). The average of these measurements is recorded 15 times per second. The drill press is set to rotate at a set speed (400 RPM unless otherwise specified), and the computer outputs a spreadsheet with two columns of relevant data, the average intensity, and the time. The test is stopped when all bitumen has been removed from the slide, or in the low temperature or high cation concentration cases, when sufficient bitumen has been removed to allow an extrapolation to be performed (a minimum of 10%).

2.2.6 Data analysis

The raw data are plotted on an XY scatter graph, and any erroneous data are removed before further analysis. This is necessary if the camera needs to be re-aimed or refocused in the first few seconds of the test, as the placement of the slide on the bracket varies slightly from run to run. This will result in artefacts in the data, which are observed

easily on the plot. Once any data cropping is complete, the average intensity of the first good reading is chosen to represent 0% recession. The final reading is chosen to represent 100% recession. All the intermediate values are scaled accordingly so that a column of data progressing from 0% to 100% can be generated. In order to make the plot less cluttered, 20 points of raw data are averaged for each point shown in the plots. A plot of percent recession vs. time is generated, and the time at which 50% recession is reached is used as a measure of the rate of recession. In the cases of incomplete recession, the final state is set to the percent recession determined optically, based on the area of bitumen remaining on the slide. Figure 2.3 shows typical recession curves generated by the algorithm.

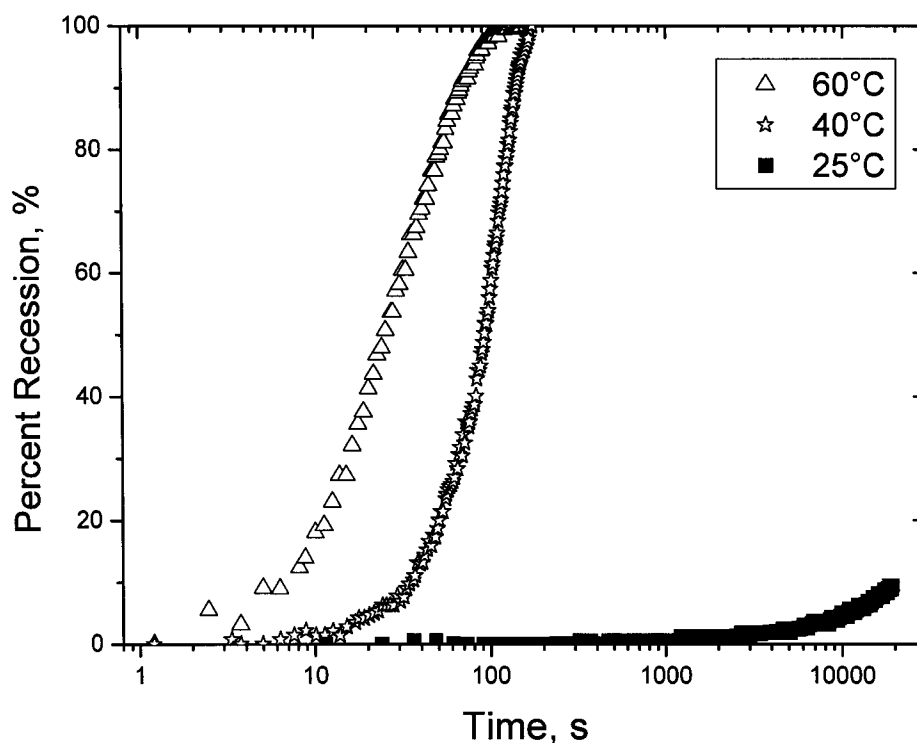


Figure 2.3 – Typical recession curves for experiments at different temperatures

2.3 Results and discussion

2.3.1 Effect of temperature

Temperature has been found to have a significant effect on bitumen recession rate. Figure 2.4 shows the averaged total time to 50% recession for samples conducted in a divalent ion free system at pH 10. As observed from the data, recession at 60°C is relatively quick, and even at 40°C there is no difficulty removing all the bitumen from the slide in a timely manner. At 25°C, however, the bitumen has never been fully recessed.

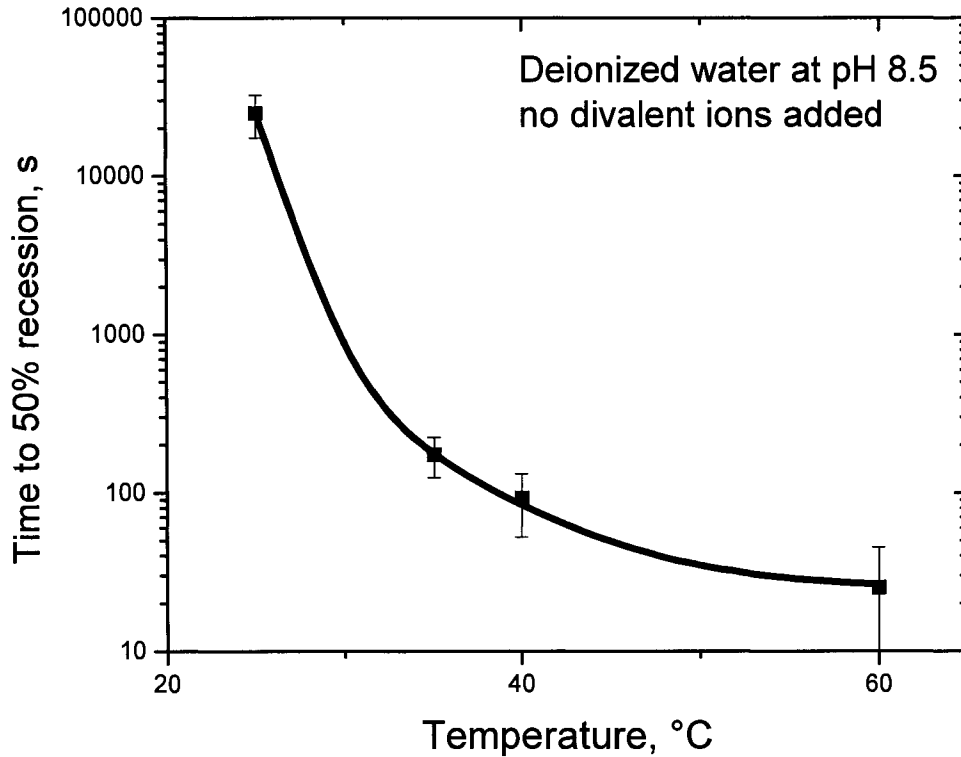


Figure 2.4 – The effect of temperature on bitumen recession

The viscosity of bitumen is highly dependant on temperature. Figure 2.5 shows the typical variation of viscosity with temperature for Athabasca bitumen. This is likely a major factor in the change in recession rate with temperature. At 60°C, bitumen flows freely, and so it is understandable that recession from the surface of the glass slide would be relatively rapid. As temperature decreases, the viscosity of bitumen increases by several orders of magnitude. At 25°C, bitumen is roughly one million times more viscous than water. At this level, the bitumen layer will be highly resistive to flow,

causing it to take a very long time to recess from the slide. This agrees with the results observed in the test.

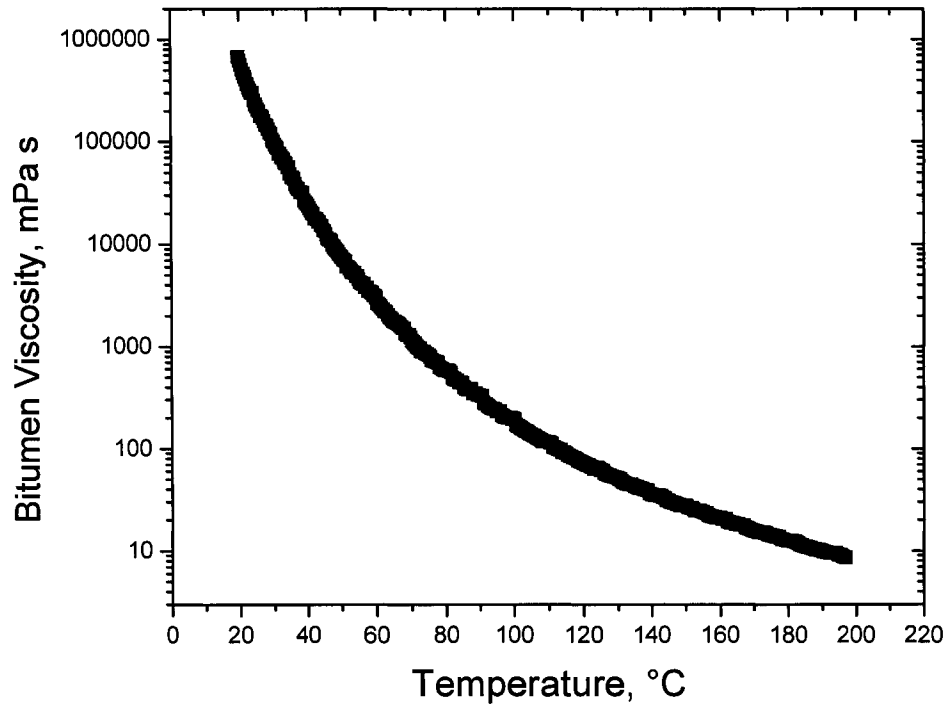


Figure 2.5 – Bitumen viscosity variation with temperature (Modified from Srinivasan, 1989)

If we combine the data from Figure 2.4 with Figure 2.5, we can plot recession time versus bitumen viscosity. This is shown in Figure 2.6. As noted in Figure 2.6, the recession time increases exponentially with respect to viscosity. We can conclude that recession time is a strong function of bitumen viscosity.

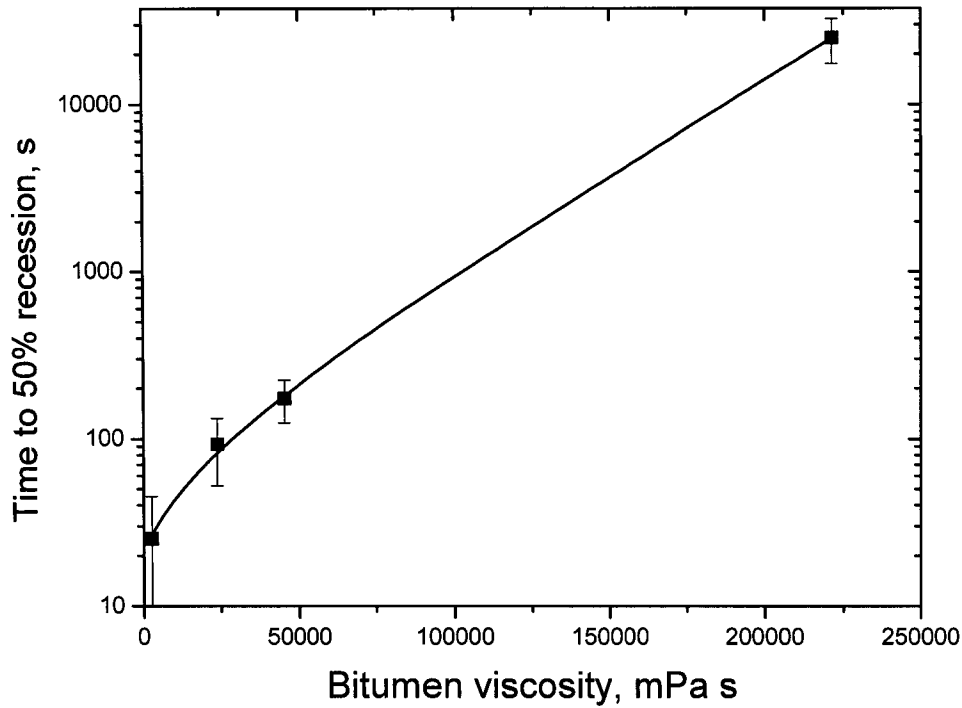


Figure 2.6 – Change in recession time with bitumen viscosity

Another factor in the change in rate of recession with temperature is the migration of surfactants from the bulk of bitumen to the bitumen surface. Figure 2.7 shows an estimation of the time required for a bitumen surface to be completely saturated with surfactants. It is clearly observed that this migration time increases by several orders of magnitude between 60°C and 25°C. These values were obtained using the Einstein-Smoluchowski equation (Hunter, 1986):

$$\langle x^2 \rangle^{\frac{1}{2}} = \left[\frac{1}{c_0} \int_{-\infty}^{\infty} x^2 c(x, t) dx \right]^{\frac{1}{2}} = (2Dt)^{\frac{1}{2}} \quad (2.5)$$

where $\langle x^2 \rangle$ is the mean squared displacement, $c(x, t)$ is the concentration profile, t is time, and D is the diffusivity, which can be estimated by:

$$D = \frac{kT}{6\pi\mu r} \quad (2.6)$$

The simplifying assumption that mass transfer is dominated by diffusion is made in order to use this equation. Consequently, the values obtained are order-of-magnitude estimates. If we assume a particle diameter of 20\AA for surfactant molecules, and a bulk concentration of 2% by mass, we can estimate the time required for the surfactant molecules to diffuse to the interface at different temperatures by using the temperature-viscosity information in Figure 2.5. Since larger concentrations of surfactants at the bitumen/water interface will increase the spread of bitumen-water-silica three-phase contact lines, the larger concentrations found at high temperature will further increase the rate of recession. While surfactants in the bulk aqueous phase are known to cause difficulties in separating oil and solid phases, the surfactants in this study should be concentrated on the interfaces, which should make the bitumen surface less hydrophobic, allowing bitumen droplets to more easily detach from the silica surface and move into the water phase.

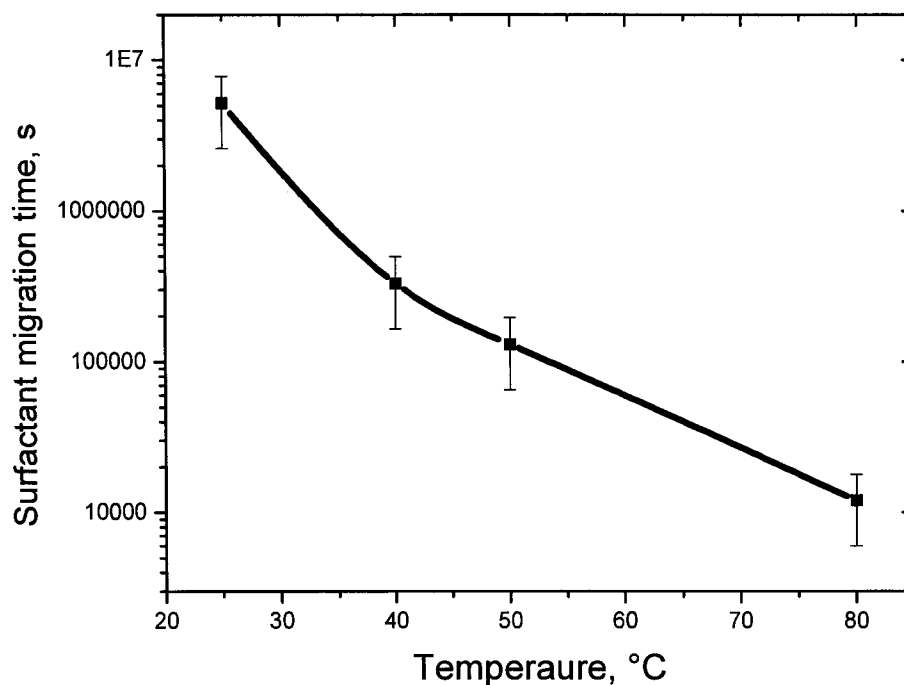


Figure 2.7 – Estimation of surfactant migration time at different temperatures

The final factor involving temperature is the effect of temperature on the double-layer forces between silica and bitumen. While these forces were not measured in this study, it

has been shown by others (Dai and Chung, 1995) that the electrokinetic repulsive force between silica and bitumen increases with increasing temperature. This would have the effect of making the glass surface effectively more hydrophilic, increasing the rate at which the oil layer recesses. Thus it is shown that all of the temperature-affected factors (viscosity, surfactant migration, and double layer forces) work synergistically to improve bitumen recession as temperature increases.

2.3.2 Effect of divalent ions

The presence of calcium ions has also been shown to have an effect on bitumen recession. Figure 2.8 shows the average time to 50% recession for solutions of deionised water at 40°C and pH 10 with varying calcium concentrations. It is shown that the time to 50% recession increases dramatically with increasing calcium concentration. With no calcium, the time to 50% recession is approximately 90 s. With addition of 25ppm Ca^{2+} from CaCl_2 , the time increases to 175 s. At 40ppm Ca^{2+} the bitumen recesses so slowly that after one hour, there was approximately 90% of the slide surface still coated with bitumen. The time to 50% recession was estimated to be approximately 6500 s by fitting the data to an exponential regression curve and extrapolating to 50%.

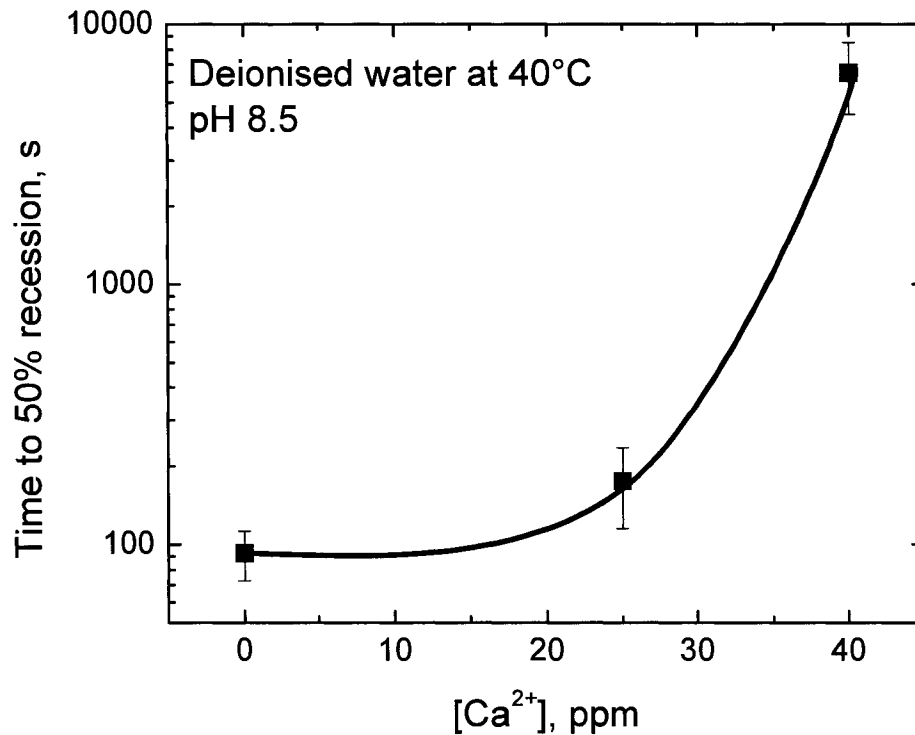


Figure 2.8 – The effect of calcium ion concentration on bitumen recession

Calcium and other divalent ions have been shown to inhibit the formation and propagation of three-phase contact lines in the bitumen-water-silica system (Basu, Nandakumar et al., 2004). Lower yields in bitumen recovery using conventional and column flotation have been consistently observed when calcium ions are present. Calcium ions act as a binder between bitumen and silica by lowering the difference in zeta potential (Liu, Zhou et al., 2002). Figure 2.9 shows the zeta potential distributions of bitumen, silica, and the two combined in a solution of 1mM KCl and 1mM CaCl₂. When bitumen and silica are combined in the presence of calcium, the two peaks merge, indicating a strong adhesion between the two surfaces (Liu, Xu et al., 2003). It is shown from the results in this study that in deionized water, calcium content has as much of an impact on recession rate as does temperature.

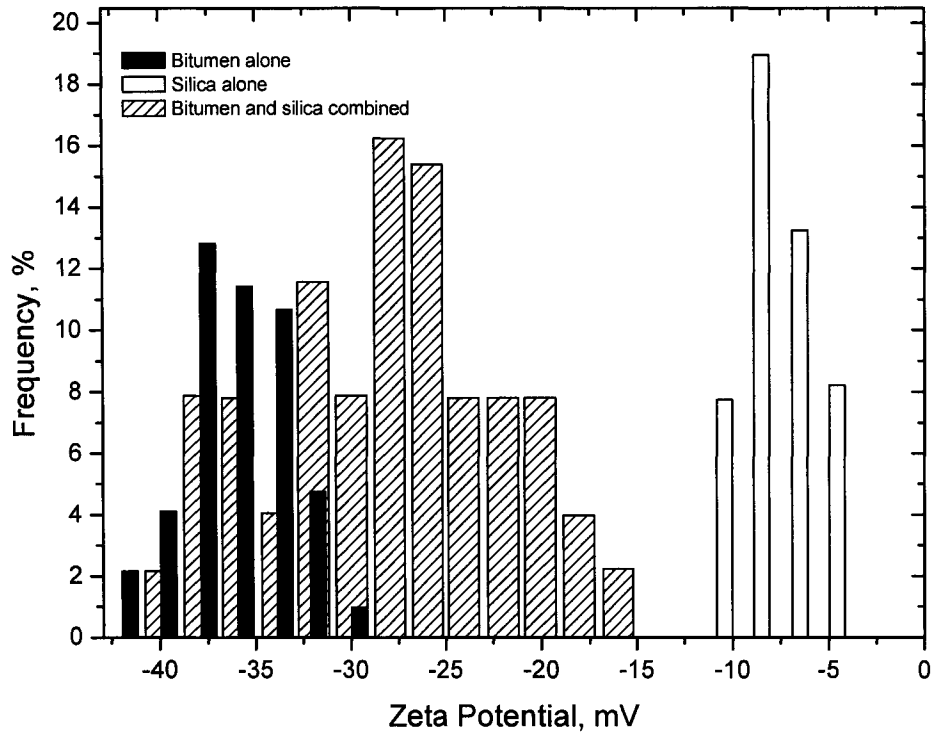


Figure 2.9 – Zeta potential distribution of the bitumen-silica system in the presence of 1 mM calcium ions (modified from Liu, Xu et al., 2003)

Magnesium ions were expected to have a similar effect to calcium ions on bitumen recession based on observations made in zeta-potential distribution measurements, interfacial tensiometry and flotation experiments. Figure 2.10 shows typical recession curves using magnesium ions as compared to calcium ions. Bitumen in the presence of magnesium is shown to recess at a rate very comparable to a test with a similar calcium mass concentration.

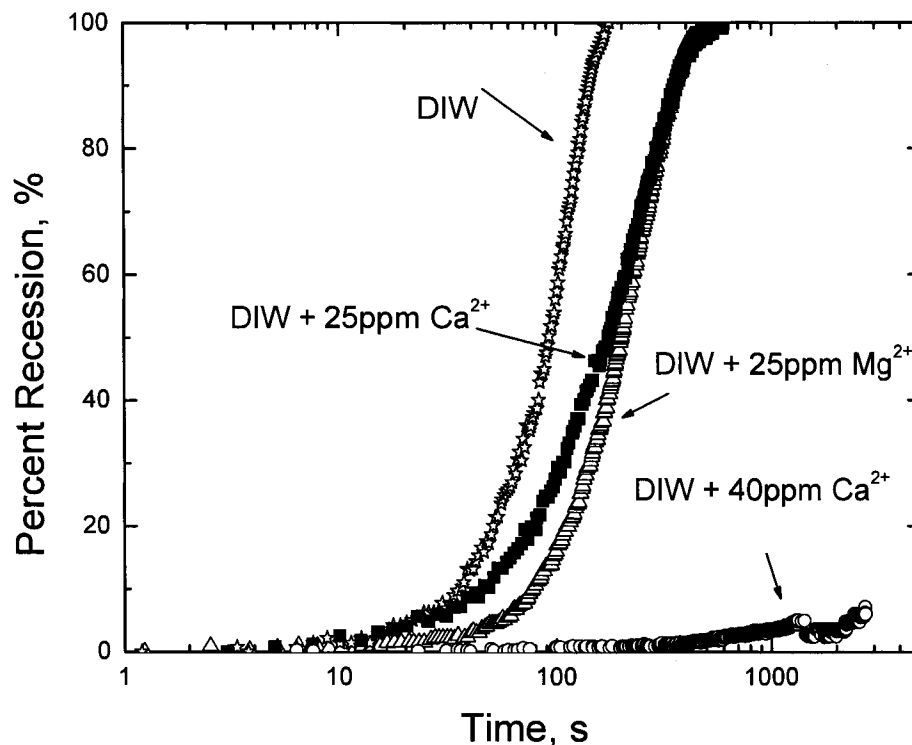


Figure 2.10 – Comparison of Calcium and Magnesium Ion Effects

2.3.3 Effect of pH

The final variable investigated in this study is the solution pH. Figure 2.11 shows the time to reach 50% recession for solutions of deionised water at 40°C without Ca^{2+} ion addition at varying pH. In general, recession occurs faster at higher pH, but the correlation is far from conclusive. Traditionally, better recoveries have been observed at higher pH values, although this is mainly due to NaOH's role in suppressing the negative effects of calcium and magnesium ions. It should be noted that the pH dependency found in this study is only valid for bitumen's release from a silica surface and should not be taken to represent an overall increase in bitumen extraction efficiency, as pH has been shown to greatly influence air-bitumen attachment, coagulation of fines and other mechanisms critical to the oil sands extraction process. It should also be noted that the effect of pH is minimal when compared to the effects of temperature and calcium ion addition. From Figure 2.11 it is noted that the change in recession times over the range

of pH's tested is about 300%, while for temperature it is four orders of magnitude, and for calcium the difference is three orders of magnitude. If we refer back to Figure 1.3 in chapter 1, we notice that at high pH, quiescent bitumen recession is slower than at low pH, but the equilibrium contact angle is higher. Therefore, in this experiment shear is present, it is logical that there is little effect of pH. At low pH, the bitumen quickly recedes to form droplets, but is more strongly adhered to the silica surface and therefore those droplets do not detach easily, whereas in the higher pH scenario, the bitumen recedes into droplets more slowly, but detaches easily once those droplets are formed. Since the hydrodynamics in the cell are inconsistent, the clear effect of pH is disguised by the experimental error. Therefore we conclude that; compared to the effect of temperature and divalent ions, the effect of pH is less significant.

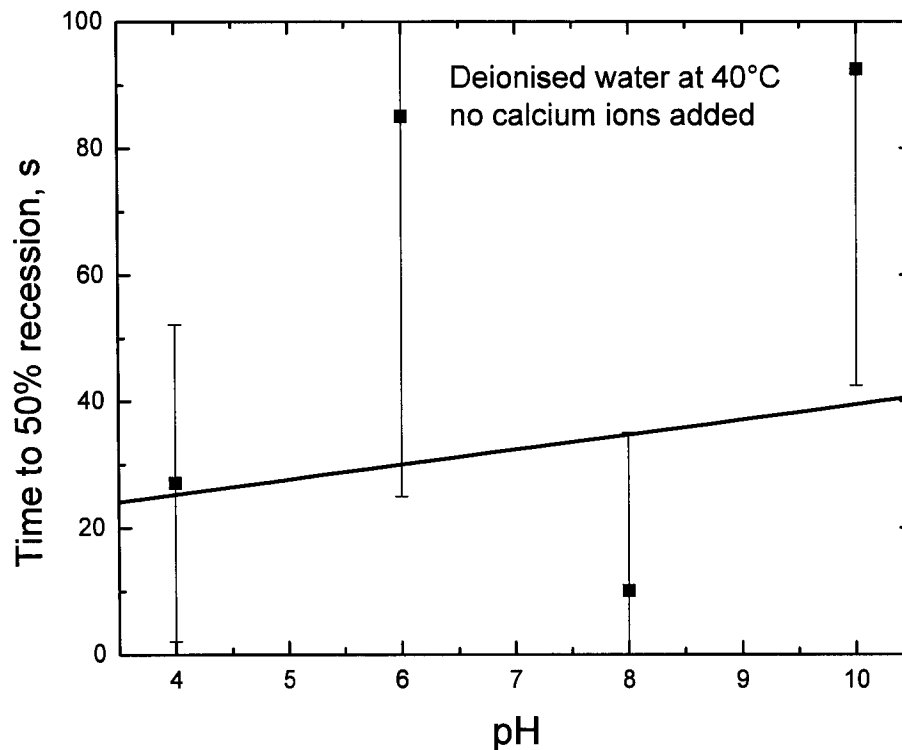


Figure 2.11 – Effect of pH on bitumen recession rate in a deionized water system

2.3.4 Industrial recycle process water

Results from laboratory-prepared solutions using deionised water with additives have been in the past criticised to not being representative of actual processing conditions. To this end a series of tests were performed using Aurora recycle process water. Detailed water chemistry information is included in chapter 3. Results from the tests at various temperatures are shown in Figure 2.12. It is noted that in general the trend is the same as in the deionized water system. However; if we compare the values with those in Figure 2.4, we note that at a given temperature the recession time is slightly higher for all conditions – that is – the slides in the process water systems recessed slower than those in the deionised water system, with no added divalent ions in solution. This confirms that the ions in the process water have an effect on bitumen recession rate, and that the process water is not optimised in terms of offering the fastest possible recession rate.

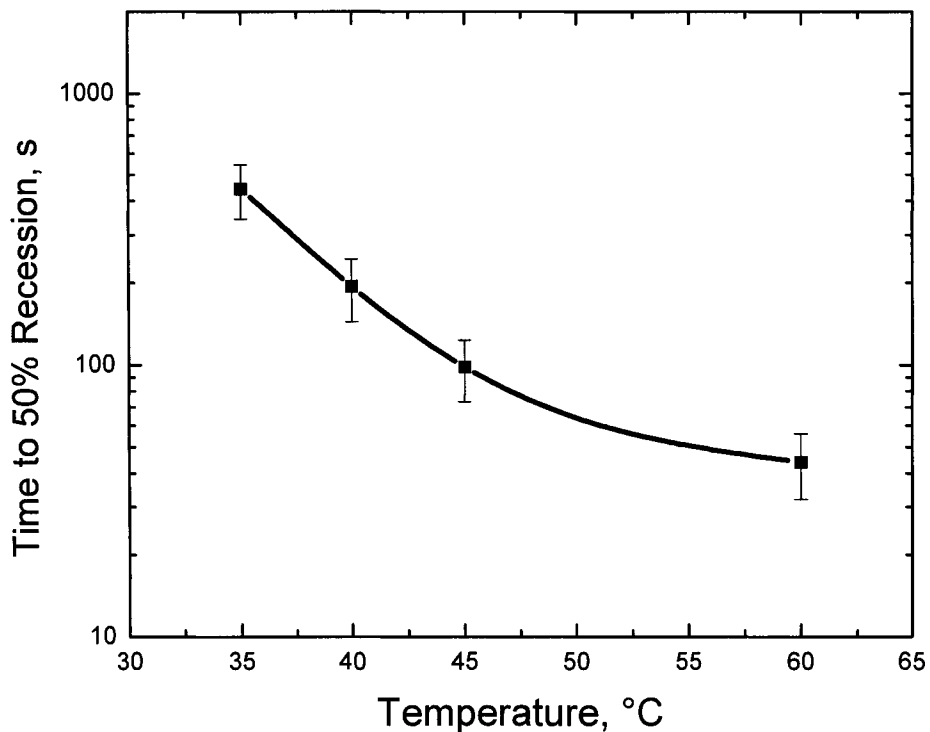


Figure 2.12 – Effect of temperature on recession in industrial process water

Figure 2.13 shows a comparison of the time to 50% recession for the process water system with the deionised water system at varying temperature, as well as one test where

deionized water was doped with the levels of sodium, chloride, sulphate, bicarbonate, calcium and magnesium ions found in the process water, referred to as ‘simulated process water’. The ‘recipe’ for the simulated process water is shown in table 2.1. It can be seen that although the process water contains significant concentrations of calcium and magnesium ions, the overall performance is better than the deionised water system with comparable ionic levels. The pH of the deionized water tests was adjusted to 8.2, to match the pH of the process water. The discrepancy in recession rate between the actual industrial recycle process water and our simulated process water is attributed to the presence of natural surfactants and bicarbonates. These surfactants have been shown to favourably influence the extraction process by suppressing the negative effects of calcium and magnesium on the formation of three phase contact lines, as well as air-bitumen attachment (Schramm and Smith, 1987). It is seen from the trends that the time to 50% recession for all water chemistries is roughly equivalent at low temperature. This is because as temperature decreases the process of recession becomes dependant on bitumen viscosity and the effects of water chemistry become less significant as the nearly solid-phase behaviour of bitumen dominates the recession rate. For this reason the process water system was not tested below 35°C, as lower temperatures would require extrapolation of the data, due to incomplete bitumen recession.

Table 2.1: Simulated process water components

Component	meq/L
NaCl	9.0
Na ₂ SO ₄	4.2
NaHCO ₃	12.5
CaCl ₂ ·2H ₂ O	2.2
MgCl ₂ ·6H ₂ O	1.6

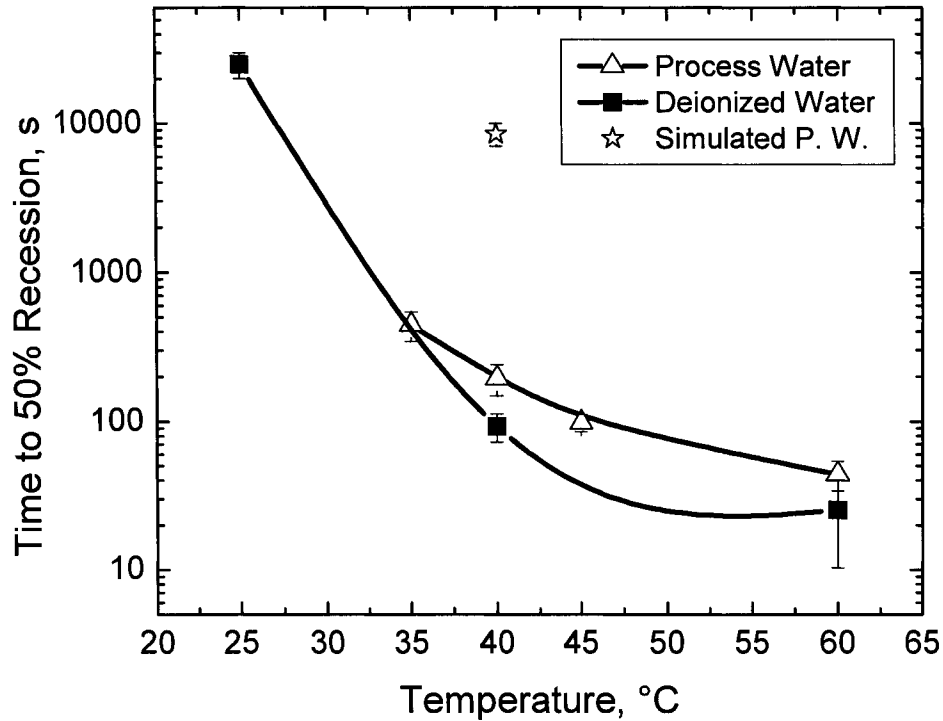


Figure 2.13 – Comparison of the process water system with the deionized water system

2.3.5 Overall results

Overall; it can be seen that the optimum recession conditions are at an above-natural pH, with no calcium or magnesium ions, and a temperature above 40°C. Since it would be nearly impossible and surely unprofitable to deionise water to process the volume of oil sands necessary on a daily basis, it is necessary to work with the water available to the industry. Thankfully, the process water contains surfactants and bicarbonates. These surfactants and bicarbonates appear to counterbalance the effects of calcium and bitumen viscosity. Thus, a balance between temperature and calcium effects and surfactant effects is required. Further study is required to determine if an optimum surfactant dosage and temperature combination exists for a process water system.

2.4 Conclusions and recommendations

From the results of this study it is shown that both temperature and calcium ion concentration play an enormous role in the rate at which bitumen recesses from a silica surface in shear flow environment. Recession rate was found to increase marginally with increasing pH, increase significantly with increasing temperature, and decrease substantially with increasing divalent ion concentration in a deionized water system. Recession rate still increased with temperature in an industrial recycle process water system. The effects of divalent ions in the process water were suppressed by the presence of natural surfactants and bicarbonates. The optimum conditions for recession in deionized water were found to be a solution without divalent ions, at as high a temperature as possible. These conditions are impractical for industrial applications, but it appears that the presence of surfactants, bicarbonates, and other chemical species in solution helps to mediate the effect of divalent ions. Further study is necessary to fully characterise the effects of surfactants and/or bicarbonates on recession dynamics. Nevertheless, the following points can be made:

- 1) Bitumen recession is strongly dependant on temperature, due to both viscous and electrokinetic effects. Bitumen recession below 35°C is a painstakingly slow process. It is unlikely that high primary recovery could be achieved by a process running below 35°C without significant support of process aids and high mechanical energy input.
- 2) Bitumen recession is also strongly dependant on calcium concentration in a deionized water system, due to the effects of divalent ions on the double layer interactions between bitumen and silica. Not only does calcium impede the recession of bitumen from the sand grains, it has also been shown to decrease the grade of the froth via slime coating phenomena. Therefore, the presence of divalent ions is doubly bad for primary extraction.
- 3) Solution pH was not found to significantly impact recession. While the optimum conditions appear at an elevated pH, there are many other factors influenced by pH in the extraction system. It is recommended that the pH should be maintained at a slightly basic level.

Chapter 3 – Recession of bitumen from a quartz surface in a channel flow device:

3.1 Introduction to chapter three

This chapter illustrates the effect of temperature, shear stress, and process water composition on the recession of bitumen from a quartz surface in a channel flow device. The experimental setup is illustrated schematically in Figure 3.1a. A detailed schematic of the flow cell is shown in Figure 3.1b, and a photograph of the cell is shown in Figure 3.2. The experimental apparatus consists of the flow cell, a variable drive gear pump, a spiral tube heat exchanger, a water bath for temperature control, a CCD camera, and a computer.

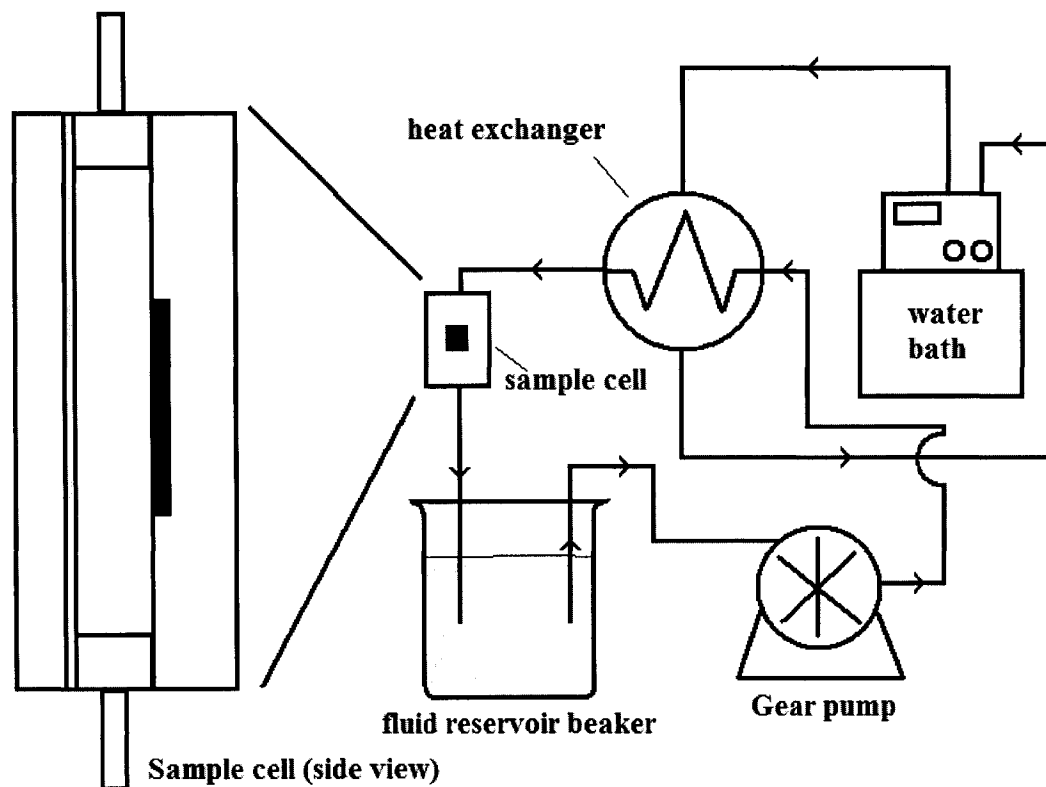


Figure 3.1a – Schematic overview of channel flow apparatus

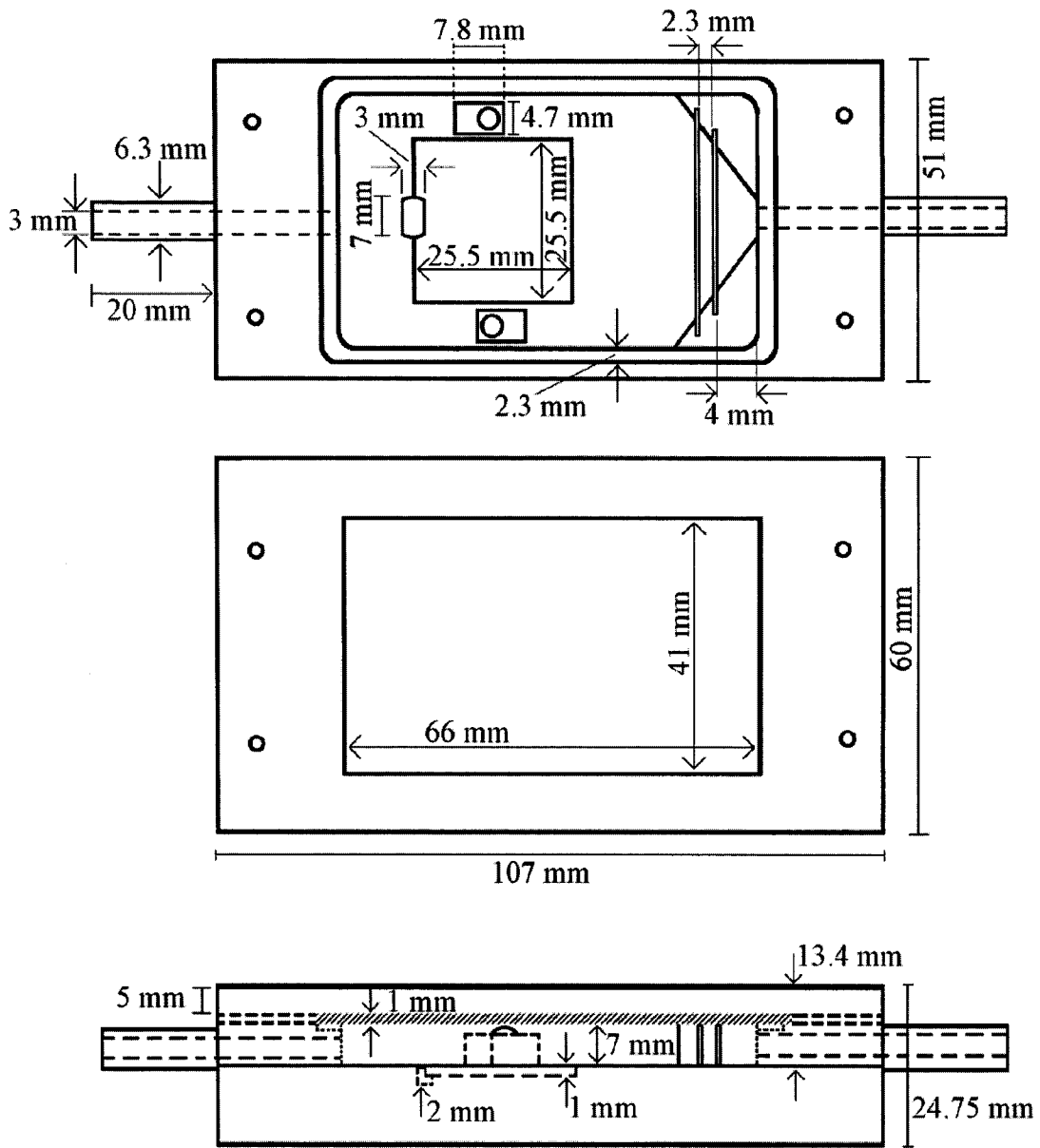


Figure 3.1b – Schematic diagram of channel flow cell – cell body, lid, and side view

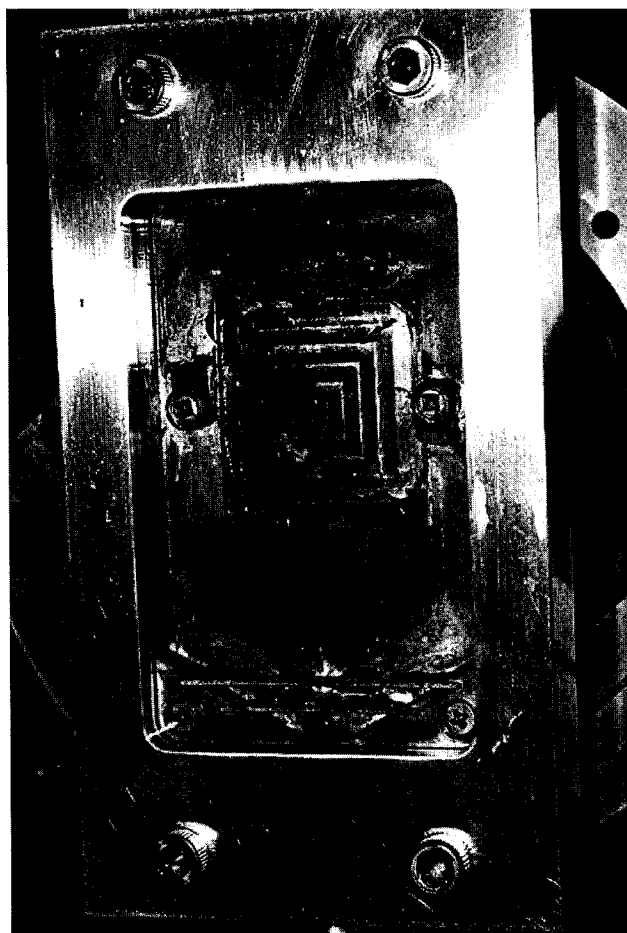


Figure 3.2 – Photographic close-up of the flow cell

Building on the results from chapter 2, a few modifications were made to the experiment. Firstly; in order to better control the hydrodynamics, the move from the couette flow apparatus to one where fluid flows directly across the slide surface was made. Secondly; the glass slides were abandoned in favour of quartz slides. While still optically transparent, these slides are advantageous as they more closely represent the surface of the sand grains found in the oil sands ore. Additionally, slides that were perfectly square were used, instead of the rectangular shape used previously, to ensure that the bitumen film created by spincoating was of more uniform thickness. Thirdly; instead of a jacketed vessel, the process liquid passes through the tube side of a spiral tube heat exchanger before entering the sample cell. The shell side of the exchanger contains a mixture of water and ethylene glycol which circulates through a temperature control bath.

In this way the temperature of the process liquid can be precisely controlled without being concerned about temperature gradients in the sample cell itself. The measurement technique – based on optical transparency of the sample slide – was the same as previously, as the stainless steel bottom to the cell was sufficiently reflective to allow the transmitted light to pass through the slide, reflect, and return to the camera.

3.2 Experimental procedure

Slide preparation, bitumen preparation, and slide coating, and data analysis were identical to those described in chapter 2.

3.2.1 Experimental preparation

In nearly all experiments performed in the channel flow apparatus, industrial recycle process water was used, and as such no chemical modifications were made to the solution. In the cases where a liquid other than industrial recycle process water was used, the preparation method was the same as described in chapter two. The singular exception to this was the set of experiments using process water foam fractions, described below.

3.2.2 Process water foam fraction preparation

Surface-active chemical species, such as naphthenic acids, are known to straddle the interface between nitrogen gas and water, as nitrogen bubbles have a hydrophobic surface. Therefore, if small N₂ bubbles are sparged through a column of process water, these surface active species should be concentrated in the froth head that forms. The de-aerated foam fraction collected via this process should have a much higher relative surfactant concentration than the residual water. To that end, a glass bubble column was constructed. The column had a diameter of 2 ¼” and a height of 34”. Four sample ports were fitted to the side of the column at 2” intervals, starting level with the top of the column, and were equipped with stopcocks. The sparger was fitted 1” from the bottom of

the column. All hose connections were sized for ¼" inner diameter tubing. A schematic illustration of this column is shown in Figure 3.3

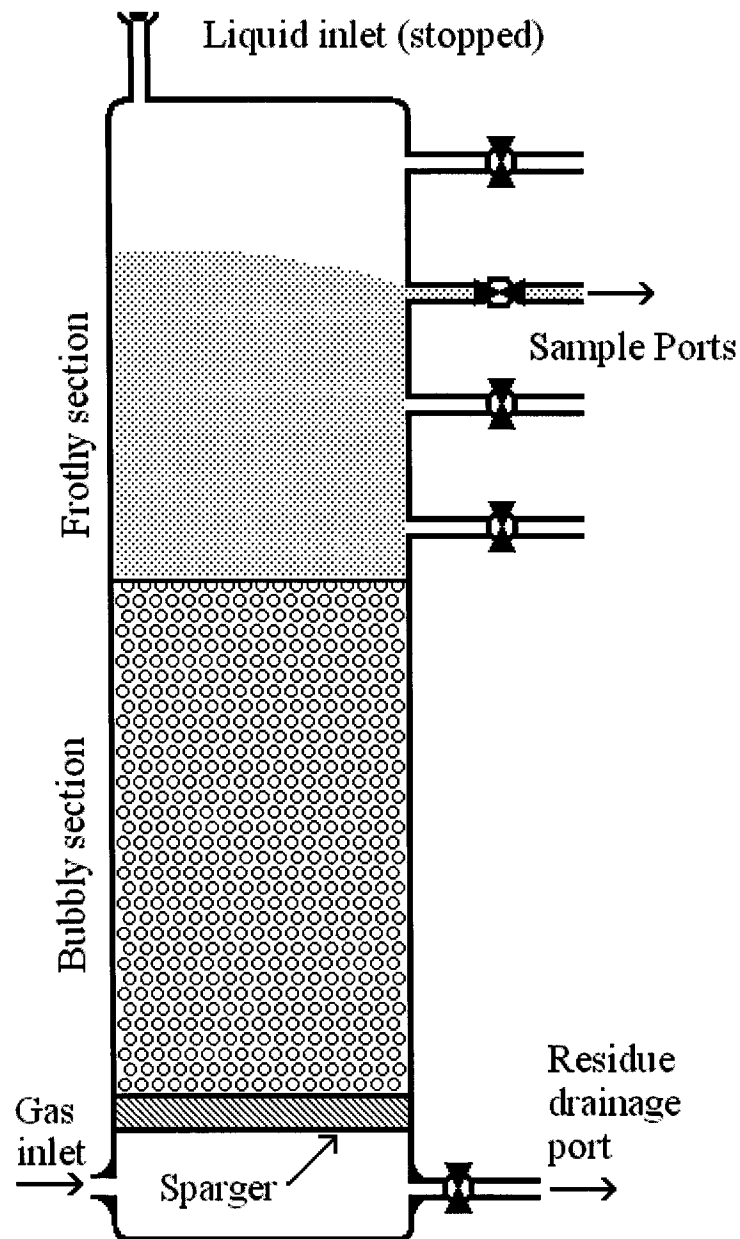


Figure 3.3 – Schematic illustration of frothing column

To generate the froth fractions desired for the recession experiment, one litre of process water was placed into the column via the inlet port in the top of the column, and the inlet port was then stopped to prevent air or froth from escaping via the inlet port. All of the

side sample ports were closed except for the top one, and water-saturated N₂ gas was allowed to flow through the sparger, generating small bubbles. The gas flowrate was adjusted to a rate such that an approximately 5cm froth head formed in the column – insufficient to allow any water to be entrained out through the sample ports. This was allowed to continue for ten minutes as a “conditioning” step, allowing the surface active materials to start to concentrate near the top of the vessel. Once the conditioning period was over, the gas flowrate was increased until the froth reached the top sample port and water began to be entrained out of the sample port. The water was collected in a clean, dry jar. This was allowed to continue until 300mL of liquid had been collected. This first 300mL is designated the “primary froth”. An additional 300mL of froth was collected in a separate jar, and was designated as the “secondary froth”. As the liquid level in the column drops due to sampling, the froth head will fall. Once the froth-gas interface drops below the level of the uppermost sample port and no more water is being entrained, the second sample port is opened and the top one is closed to allow further froth to be collected. This ensures that the froth collected is always from the top of the froth head. Once the secondary froth is collected, the flow of N₂ is stopped, and the residue drainage port is opened, allowing the residual water to be collected into a third jar. This liquid is designated the “residue”.

Since the experiment requires more than the 300-400mL of liquid collected from each run, additional frothing runs are conducted until a sufficient quantity of froth water is collected.

3.2.3 Experimental

The volume of solution needed in this experiment was much larger than in the previous experiments, due to the volume of the pump head, heat exchanger, surge beaker, and all the connecting hoses, consequently 3 litres of solution was prepared in each case. Before starting an experiment, the surge beaker was cleaned thoroughly and roughly 1.5 litres of solution was pumped through the equipment and into a waste bucket in order to flush out the system. The remaining 1.5 litres was then pumped through the system, but was

captured in the surge beaker, and then allowed to circulate continuously. The temperature control bath was then set to the desired setting, and both the heating fluid and the process fluid were allowed to circulate until their temperatures equalized at the desired level.

Once the process liquid had reached the desired temperature, the bitumen-coated quartz slide was inserted into the sample cell by first draining the process liquid, then removing the cover glass, then inserting the slide. The cover glass was quickly replaced and the cell re-filled with process liquid. The camera was focused on the slide's surface and the viewing light was turned on. At this point the computer data acquisition process – identical to that used in Chapter 2 – was initiated and the pump was set to the desired flowrate and allowed to run until the test was complete.

After the completion of each test, the process fluid was discharged from the system and roughly 4 litres of deionized water was pumped through the equipment to flush out the remaining process liquid.

3.3 Results and discussion

3.3.1 Test for reproducibility

The first set of experiments performed with the channel flow apparatus were a set of three four-slide batches, over the course of several days, all under the same experimental conditions. These were conducted in order to test the reproducibility of the experimental runs, and compare them to previous testing. The results are shown in Figure 3.4. All of the experiments in this series were performed at a temperature of 42°C, with a liquid flowrate of 2.2 litres per minute. This flowrate was chosen arbitrarily, as it is the 50% setting on the pump, and was used as the baseline flowrate throughout the experiment.

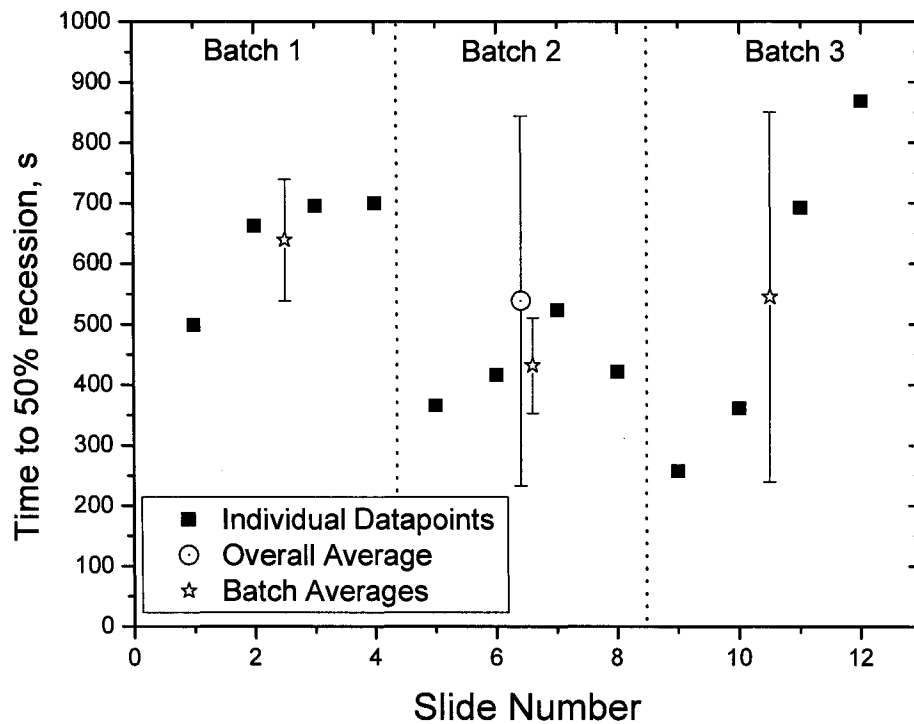


Figure 3.4 – Time to 50% recession for 12 individual slides

As observed, the data are relatively evenly scattered about the mean, similar to the experimental error observed in the previous tests described in chapter 2. The scatter is likely due to slight variations in the thickness of the bitumen film from slide to slide. Since the total mass of bitumen deposited in the film is small compared to the mass of the slide itself, we are unable to precisely measure the bitumen film thickness to discern if the variation we observe is solely dependant on variations in film thickness, or if there are other factors at play. Since the slides used in this experiment are larger than those used previously, the variation in film thickness is likely larger than with the smaller glass slides. Therefore, even with the better controlled hydrodynamics of this cell, the reproducibility of this experimental apparatus is comparable to the previous rotating coaxial cylinder tests.

It should be noted that the time to 50% recession in the channel flow system is markedly higher for any given temperature than that found in previous tests. For instance, the

average time to 50% recession for a process water system at 40°C in the rotating cylinder apparatus was approximately 200 seconds, while in the channel flow apparatus is approximately 550 seconds. This is attributed to the lower shear stress in this cell, and the larger surface area of bitumen to be recessed. Also, the change from a glass surface to quartz may have an influence on the recession rate. Therefore, we cannot directly compare the results from the two different apparatus. We can, however, compare the trends observed in the two apparatus.

3.3.2 Effect of temperature

A set of experiments was performed at varying temperature. These experiments were performed primarily to validate that the new equipment was capable of replicating the trends observed previously.

Figure 3.5 shows the time to 50% recession for experiments at three different temperatures using the channel flow apparatus. Aurora recycle process water was used in all experiments. It can be observed on the plot that, although the recession is slower in the channel flow apparatus, the trend with respect to temperature is identical. Therefore, we can confidently use the channel flow apparatus as a tool to investigate bitumen recession from a quartz surface.

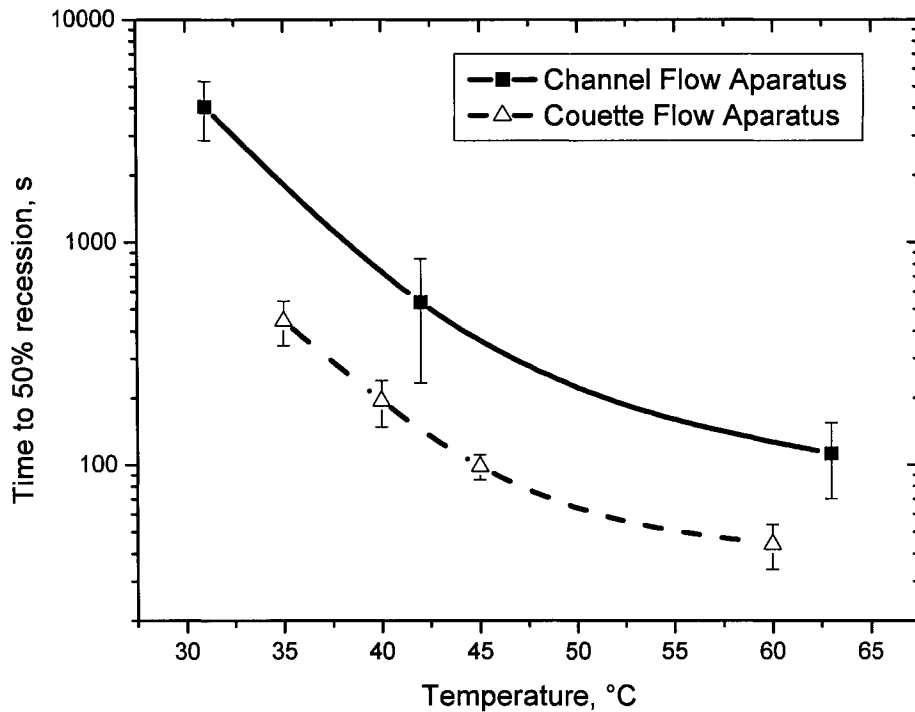


Figure 3.5 – Effect of temperature on bitumen recession

3.3.3 Effect of shear

One of the advantages of the channel flow apparatus over the coaxial device is that the shear stress is precisely controlled and can be easily varied by simply altering the flowrate of the pump. First, the Reynolds number is calculated from the flow rate, according to equation 3.1 (Bird, Stewart et al., 2002). The viscosity of water is approximately 0.65 mPa·s at 42°C, and the density is approximately 990 kg/m³. Since the exact composition of the process water is not known, approximate values for the density and viscosity will be used in the calculation of Reynolds number.

$$Re = \left[\frac{l_o v_o \rho}{\mu} \right] \quad (3.1)$$

where Re is the dimensionless Reynolds number, l_o is the characteristic length – taken to be the depth of the flow channel – v_o is the average velocity, which can be calculated by

dividing the volumetric flowrate by the cross-sectional area of flow, ρ is the fluid density, and μ is the fluid viscosity. The shear stress at the wall for flow over a flat plate is defined by equation 3.2 (Fox, McDonald et al., 2004).

$$\tau_w = \mu \left. \frac{\partial u_x}{\partial y} \right|_{y=0} \quad (3.2)$$

Using the Blasius power series expansion, Fox, McDonald et al., 2004 showed that:

$$\tau_w = \frac{0.332 \cdot \rho U_\infty^2}{\sqrt{\text{Re}_x}} \quad (3.3)$$

Table 3.1 shows the Reynolds numbers and shear stresses calculated for three experimental flowrates tested in this study. Since the critical Reynolds number for flow over a flat plate is between 1×10^5 and 3×10^5 , the flow is laminar in all cases for this experiment. While the cell is not long enough to achieve fully developed flow, the slide is mounted to the wall. Therefore the fact that the top and bottom boundary layers do not intersect should not significantly effect recession.

Table 3.1 – Reynolds numbers for various flowrates

Flow Rate – L/min	Reynolds Number	Shear Stress - Pa
1.0	2250	0.023
2.2	4940	0.076
4.0	8986	0.187

Figure 3.6 shows the average time to 50% recession versus volumetric flowrate. As noted, the recession rate increases with increasing flowrate. This is not surprising, as the shear stress is proportional to the flowrate. While the film rupture and recession into droplets should be minimally affected by the shear stress, the rate at which bitumen droplets are removed from the slide's surface will be greatly increased at higher flowrates. All experiments were performed in aurora recycle process water at a temperature of 42°C. Presented for comparison is the recession time and shear stress for the couette flow device discussed in chapter 2. It is observed that the recession is

considerably faster in the couette flow device, even though the shear stress is comparable to the moderate flow rate setting. It is apparent that shear in turbulent flow is more effective for bitumen recession than shear in laminar flow.

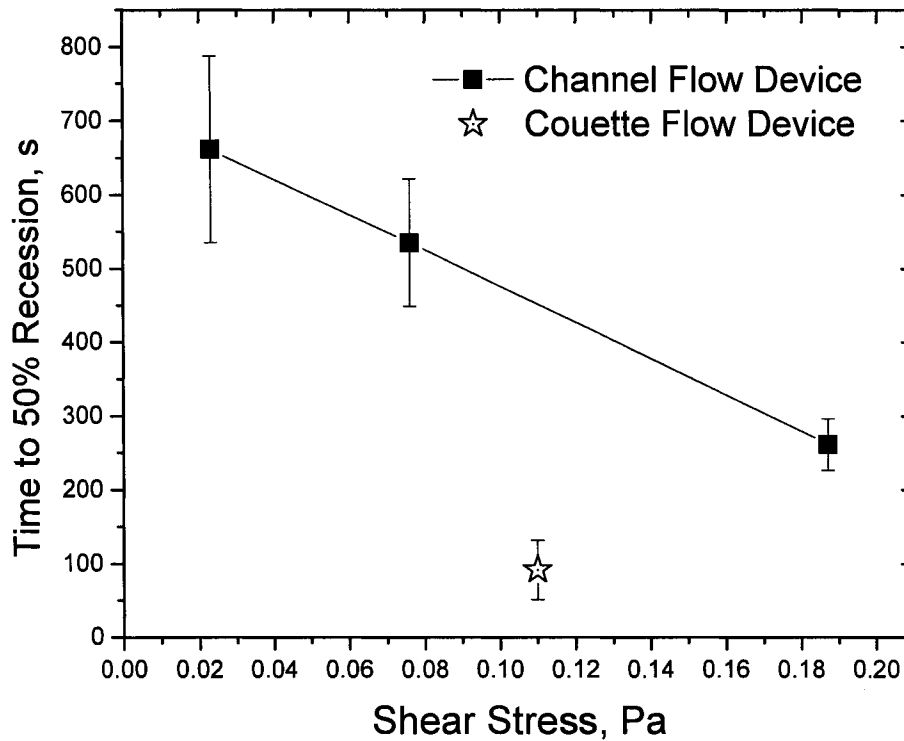


Figure 3.6 – Effect of shear stress on recession rate

3.3.4 Effect of process water composition

The term “process water” is used frequently in the field of oil sands extraction, with little regard to the exact nature of this water. We know that the process water supplied to us by Syncrude Canada Ltd contains significant quantities of inorganic ions - sodium, potassium, calcium and magnesium, as well as carbonates, bicarbonates, chlorides, sulphates, and nitrates. It also contains naphthenic acids and other surface active species. Suspended in the water are fine clay and silica particles, as well as microscopic emulsified oil droplets. The majority of these chemical species come from the exposure to the oil sands ore. As the exact composition of the oil sands ore can vary significantly

from one shovel-scoop to the next, the process water is surely to also vary in the nature and composition of the species dissolved or suspended in it. To that end, a series of tests were conducted in order to determine what effect, if any, the exact nature of the process water had on the recession rate of bitumen from a quartz surface.

3.3.4.1 Effect of process water foam fractions

Recession experiments were performed in process water froth fractions, collected via the procedure described above. The primary foam fraction was found to have a surface tension of 54 mN/m, while the residue fraction had a surface tension of 66 mN/m, compared to a surface tension of 70 mN/m of the whole process water. The variance in surface tension confirms that surface-active species are being concentrated in the froth fraction. In each case, the process water was heated to a temperature of 51°C for the experiment. Figure 3.7 shows the results.

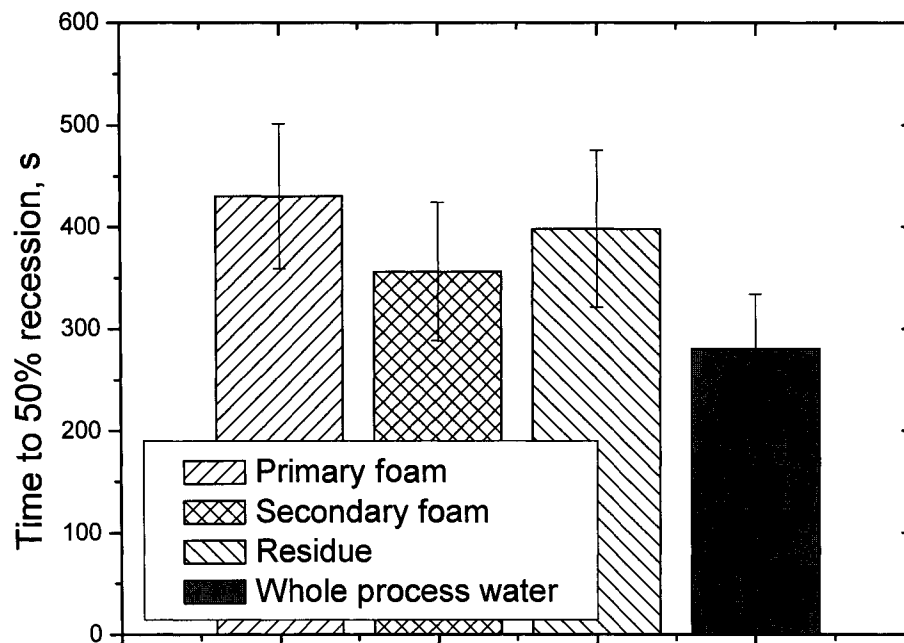


Figure 3.7 – Recession of bitumen in process water foam fractions

It is observed that the primary foam fraction, secondary foam fraction, and residue fraction do not show significantly different time to 50% recession, and are not significantly different than the unaltered process water. Additionally, if you look at the recession curves themselves – presented in Figure 3.8, the curves for the three different fractions are observed to overlap throughout the entire 0-100% range. Therefore, it is concluded that the foam fractionation of the process water does not significantly effect recession. It is likely that although the relative concentration of surfactants is higher in the foam fraction of the process water, the remaining quantity in the residue is sufficient for good recession, and the additional quantity in the froth does not further enhance recession. Further study is needed to determine what the critical minimum surfactant concentration for recession is; or if indeed such a value exists.

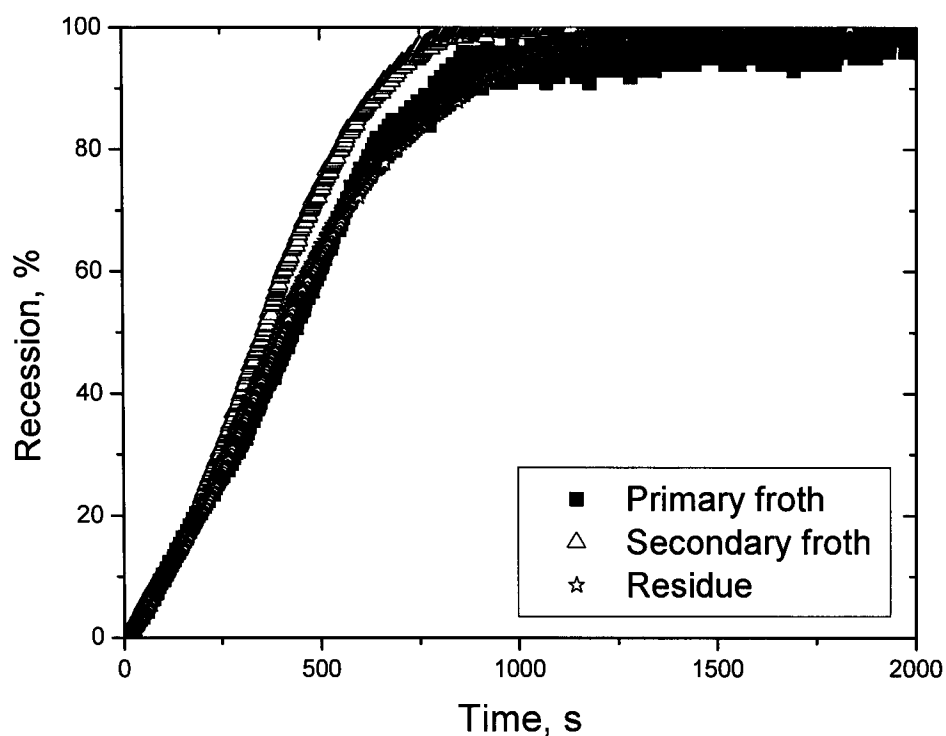


Figure 3.8 – Recession curves for process water foam fractions

3.3.4.2 Effect of process water source

The process water used throughout the experiment up to this point has been Aurora industrial recycle process water (also known as “Aurora EXP process water”), supplied by Syncrude Canada Ltd. An additional process water sample was obtained from Albian Sands, Inc., and recession tests were performed in both waters for comparison. Albian Sands, Inc. uses a process very similar to Syncrude Canada Ltd in order to extract their bitumen, except their process does not use sodium hydroxide in extraction and uses a different process to treat their froth. In the Albian process, a paraffinic solvent is used, which causes a portion of the very high molecular weight hydrocarbons to precipitate out. Since water is removed in the froth treatment process and all process effected water eventually ends up in the tailings pond and ultimately in the recycle water, there may be some differences in the process water due to the differences in the froth treatment process, in addition to the variations due to the geographic location of the oil sands ore.

Figure 3.9 shows the average time to 50% recession for recession experiments in the two different process waters. While it appears that recession is slightly faster in the Albian Sands industrial process water, the two values are within the experimental error of each other. Therefore the difference in recession rate between the two water samples is not significant. Even if the error bars were smaller, the difference between the two is only 10%, which when compared to the changes observed with temperature, divalent ion content, or shear stress, is minimal.

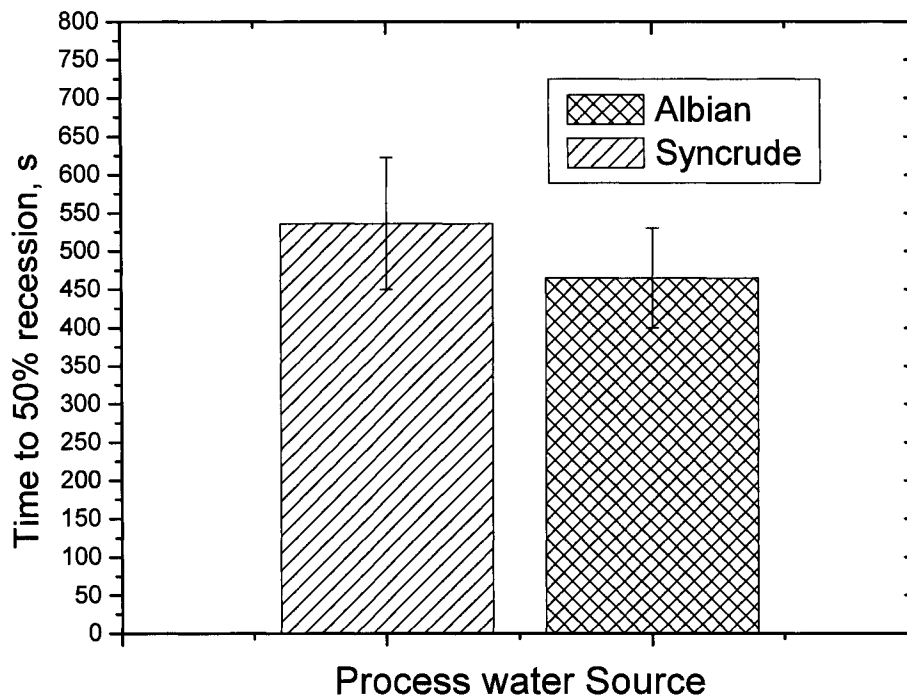


Figure 3.9– Recession rate for differently sourced process waters

As we have noted in chapter two, ion concentration and pH can have an effect on bitumen recession. Therefore the two different waters were tested to see if there were any significant differences between them in ion concentration and pH. Samples of each type of water were submitted to the Natural Resources Analytical Laboratory at the University of Alberta for analysis by ion chromatography. The results of these tests are shown in table 3.2. It is observed that the concentrations of nearly all ions is lower in the Albian sands process water, especially calcium and magnesium ions. Albian sands does not dope their extraction process with sodium hydroxide, resulting in the substantially lower sodium ion content. The lack of NaOH may also be responsible for the marginally lower pH. It is possible that the lowered calcium and magnesium ion content observed in the Albian water is responsible for the slight reduction in recession time observed in Figure 3.9.

Table 3.2 – Water chemistry of industrial process water samples

Ion concentration (ppm)	Syncrude	Albian
Sodium (Na ⁺)	503.3	236.2
Potassium (K ⁺)	14.3	15.0
Calcium (Ca ²⁺)	48.4	15.5
Magnesium (Mg ²⁺)	18.9	9.0
Chloride (Cl ⁻)	431.3	116.8
Nitrate (NO ₃ ⁻)	1.48	0.3
Sulfate (SO ₄ ²⁻)	63.06	25.8
Bicarbonate (HCO ₃ ⁻)	646.6	418.9
pH	8.2	7.8

3.3.4.3 Effect of surfactant co-precipitation with calcium carbonate

In chapter 4, process water which was heated above 80°C was shown to form a precipitate which, while consisting primarily of calcium carbonate, depleted natural surfactants from the process water solution (Choung, Walker et al., 2004). Therefore, it was desired to determine what effect this “surfactant-depleted” process water would have on a recession experiment. Figure 3.10 shows the average time to 50 % recession for experiments performed using the “depleted” process water, as compared to unaltered process water. A thorough explanation of the procedure used to deplete the process water, as well as isolation and identification of the precipitate can be found in Chapter four.

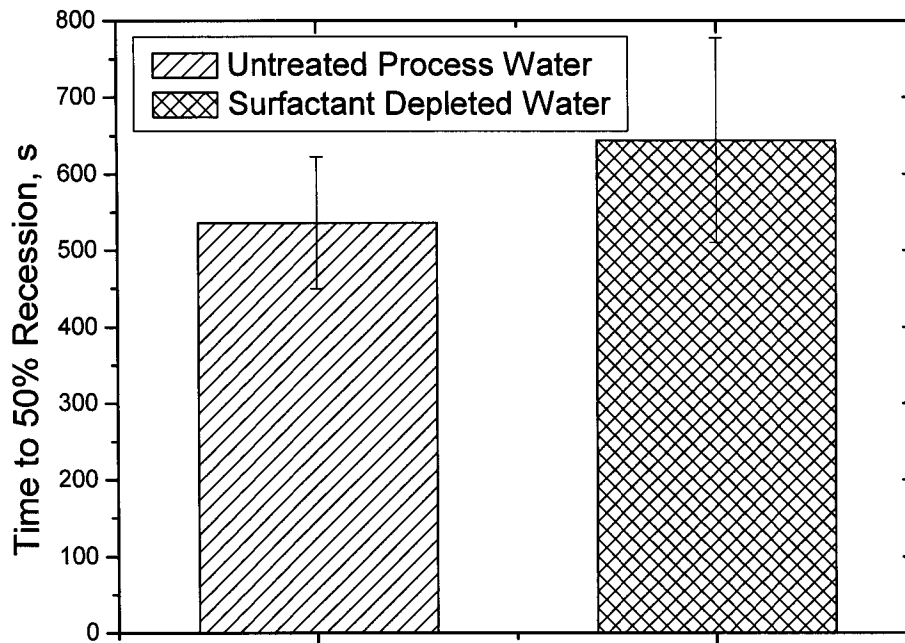


Figure 3.10 – Effect of surfactant depletion by co-precipitation on bitumen recession

As observed in Figure 3.10, recession experiments performed in industrial process water that has had a portion of its surfactants removed by co-precipitation with calcium chloride were, on average, approximately 20% slower than in process water which had not been treated. However, the difference was on the same order of magnitude as the experimental error. Similar to the case of process waters of different sources, and the process water foam fractions, the difference in recession time is small when compared to the effect of temperature or flow rate.

3.3.5 Oil sand ore

In a related experiment, an attempt was made to analyse the recession of bitumen from oil sand ore *in situ*. It was desirable to use oil sand ore in an effort to compare our model system with ‘real’ recession processes. Another cell, similar in construction to the channel flow apparatus, was constructed. The primary difference was that the ‘pocket’ in the bottom of the cell was deeper, to allow a small quantity of oil sand ore to be pressed into it. Due to the thickness of the oil sand cavity, a second heating channel was also

included in the cell, to ensure the oil sands ore was maintained at a uniform temperature. The magnification of the optical system was increased, so that the camera was focused on a small number of individual bitumen-coated sand grains. The experimental setup is shown schematically in Figure 3.11.

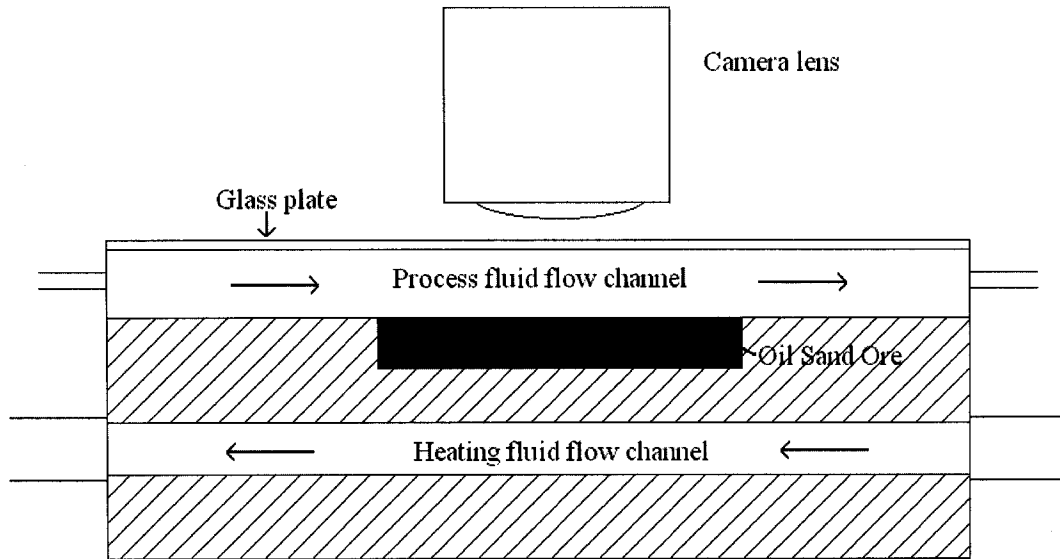


Figure 3.11 – Modified sample cell for oil sands ore

A number of unforeseen difficulties arose during the use of the oil sands ore cell. Firstly; the intensity of light reflected from the sand grains once bitumen had recessed was not sufficiently different from the intensity of light reflected from the bitumen surface itself. While almost no light reflects from the bitumen, the sand grains were not very reflective either. This is partly because instead of having a reflective plate of stainless steel behind them as in the slide case, there are simply more bitumen-coated sand grains. Secondly; once bitumen had receded from the top layer of sand grains, those sand grains were no longer well adhered to the sample cell and broke free. This not only exposed fresh bitumen – causing an apparent drop in recession – but the sand grains got into the pump and causes mechanical problems. The recession curve for one run with the oil sand ore is shown in Figure 3.12.

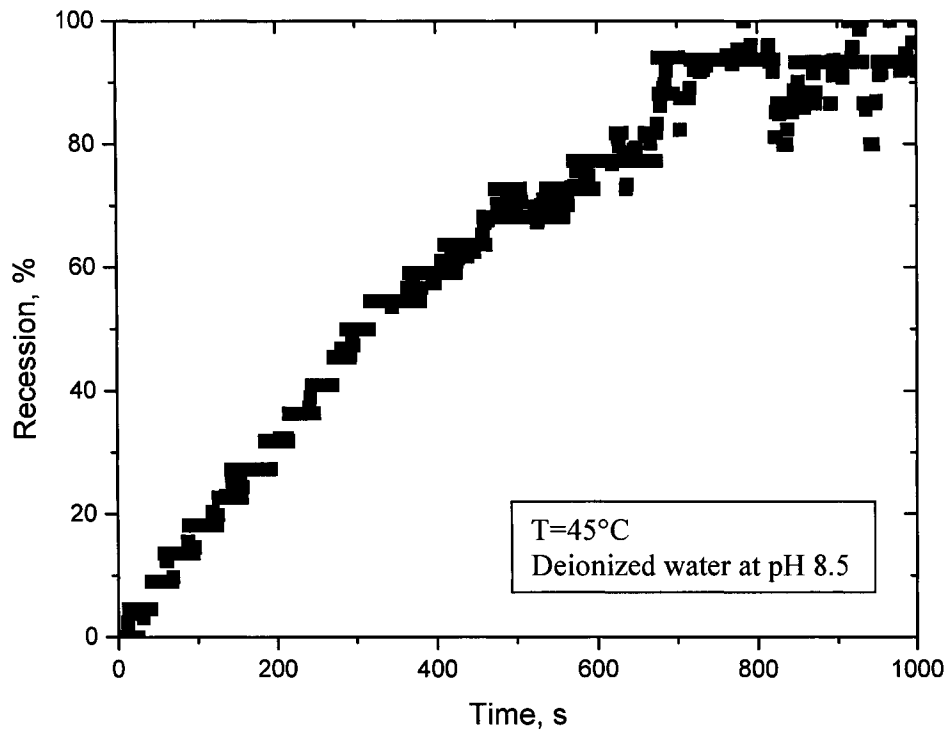


Figure 3.12 – Recession of bitumen from oil sand ore – observed *in situ*

It is observed that while the curve follows the same general shape of the slide-based experiments, the recession appears to increase ‘stepwise’ in a series of jumps. This is an indication of poor contrast. Since the greyscale intensity is measured on a scale from 1-255, if the difference between the start intensity and the end intensity is only 30-40 points, the calibrated recession curve will appear this way. Additionally, the ore disintegration can be observed in the data. Two distinct downward spikes can be seen at approximately 850s and 950s, respectively, indicating that at that time, one or more sand grains broke free, exposing a darker surface to the camera. Clearly, the current experimental setup is not adequate for observing the recession of bitumen from oil sand ore *in situ*.

3.3.6 Overall results

Overall, the channel flow apparatus performs comparably to the coaxial cylinder device, while occupying a much smaller laboratory footprint. The variation in recession rate with temperature was found to mirror the results found in chapter two, although the recession at all conditions was found to be slower. The two are not directly comparable, however, as the flow regime in the channel flow cell and the couette flow cell are not the same. The fluid flowrate (and therefore shear stress) was found to have an effect on bitumen recession, with faster recession occurring when the fluid flowrate was higher. The recession rate of bitumen from a silica surface was found to vary slightly for the two different types of industrial process water, but the variation was found to be within the experimental error. Concentrating the surface active materials present in the process water into a foam fraction did not noticeably enhance recession, nor was recession noticeably impaired in the surfactant-depleted residue fraction. Removal of surfactants by the co-precipitation method discussed in chapter four also did not significantly affect the rate of recession. An attempt to measure the recession of bitumen from the surface of oil sand ore sand grains in situ was impaired by a lack of optical contrast, and the disintegration of the oil sand ore.

3.4 Conclusions

The results of this chapter show us that the channel flow apparatus is a powerful tool for investigating the effect of process variables on the recession of bitumen from a silica surface. The accuracy of the channel flow device is similar to the coaxial cylinder device used in chapter two, but occupies a much smaller space in the laboratory, as it does not require a large device, but rather a small gear pump as the source of mechanical energy. Bitumen recession was found to occur faster at higher fluid flowrates, and vary slightly with varying process water composition. Changes in the exact composition of the process water used did not significantly effect recession. The key results from this chapter can be summarized as follows:

- 1) The accuracy of the coaxial cylinder device and the channel flow device was found to be comparable. Recession occurred slower at all conditions in the channel flow device, despite the fact that the shear stress in the coaxial cylinder device was less than in the channel flow device at all flowrates tested. The flow was turbulent in the Couette flow case, and laminar in the channel flow case.
- 2) Bitumen recession is dependant on shear stress. Recession was found to be faster with higher volumetric flowrate – and therefore higher shear stress– and slower with lower flowrate. This was attributed to the larger drag force exerted by the fluid on the bitumen film in a higher shear environment. Shear in turbulent flow – as in the couette flow case – was found to be more effective for bitumen recession than shear in laminar flow.
- 3) Process water composition had little effect on bitumen recession. While the chemistry of process water samples from two different sources varied, the recession rates obtained using the different solutions was comparable.
- 4) Separation of process water into a surfactant-rich foam fraction and a surfactant-poor residue fraction did not significantly affect the recession rate. Recession rate in the process water fractions was found to be similar to that of unaltered process water.
- 5) Process water that has been heated above 80°C to trigger calcium carbonate precipitation and surfactant depletion showed a mild increase in recession time when compared to unaltered process water.
- 6) Observation of recession of bitumen from the surface of oil sand ore was not successful using the current experimental setup.

Chapter 4 - Effect of temperature on the stability of froth formed in the recycle process water of oil sands extraction¹

4.1 Introduction to chapter four

In previous chapters we have looked solely at the effect of temperature and water chemistry on the recession rate of bitumen from a silica surface. This chapter deals with the effect of temperature on the water chemistry itself. During the course of the tests performed in this work, a previously unobserved phenomenon was discovered, where changes in temperature causes irreversible changes in process water composition. This chapter investigates this phenomenon.

As the world supply of conventional oil reserves dwindles, the economic importance of Canadian Athabasca oil sands deposits becomes ever greater. Currently, bitumen extracted from the Athabasca oil sands accounts for over 25 % of total oil production in Canada. Both Syncrude Canada Ltd. and Suncor Energy Inc. are among the pioneers in commercial exploration of the Athabasca oil sands using the Clark Hot Water Extraction (CHWE) process (Baptista and Bowman, 1969; Hepler and Smith, 1994). This process involves mixing oil sands ore with hot water in a mechanical tumbler or in a hydrotransport pipeline, in which bitumen liberation from sand grains takes place. Small quantities of caustic, commonly sodium hydroxide, are added to the slurry to neutralize organic acids in the bitumen and produce surfactants (Sanford and Seyer, 1979). The surfactants lower the interfacial tension between the bitumen and the aqueous phase of the oil sands slurry, leading to the formation of a three phase bitumen-water-solid contact line, from which the bitumen recedes to form a drop and eventually detach from the sand grains. The bitumen droplets then attach to air bubbles generated by aeration of the

¹ A version of this chapter has been published. Choung, J., J. Walker, et al. (2004). "Effect of temperature on the stability of froth formed in the recycle process water of oil sands extraction." *Canadian Journal of Chemical Engineering* **82**(4): 801-806. This chapter is based on initial theoretical work performed by Dr. J Choung. All experimental tests and data analysis were performed by J. Walker. The first draft of the text was prepared by J. Walker and the final text was submitted for publication in the Canadian Journal of Chemical Engineering by Dr. J. Choung.

slurry. The aerated bitumen droplets float to the top of the slurry to form a bitumen-rich froth in a primary separation vessel. The bitumen droplets remaining in the slurry are further recovered using conventional mechanical flotation cells.

Athabasca bitumen is a complex hydrocarbon mixture containing varying levels of metal ions and water-soluble surfactants (Moschopedis, Fryer et al., 1977; Ali, 1978; Schramm and Smith, 1987). The water-soluble species released into the aqueous phase during the extraction process play an important role in bitumen flotation. These species interact with solids, water, bitumen and air bubbles in a complex manner. Schramm, Smith et al., 1984 reported that the surfactants make the air bubbles and bitumen droplets more hydrophilic, resulting in poor air-bitumen attachment. The adsorption of surfactant onto solid particles increases the solid-air attachment, resulting in poor froth qualities (Baptista and Bowman, 1969; Ignasiak, Zhang et al., 1985; Kotlyar and Sparks, 1985; McIntyre, Montgomery et al., 1985). However, the controlled release of natural surfactants is essential not only for facilitating bitumen liberation, but also for achieving a higher recovery in bitumen flotation. Zhou, Xu et al., 2000 investigated the effect of natural surfactants on air hold-up, defined as the volume fraction of the pulp occupied by air bubbles generated in a flotation vessel. They found that under ambient temperature the air hold-up in the resultant supernatant of the conditioned oil sands slurry was much higher than that in de-ionized water. A further increase in air hold-up was observed with the supernatant obtained from the oil sands slurry conditioned with caustic. The aging of the ore prior to bitumen extraction also caused an increase in air hold-up by increasing the natural surfactant concentration. It is evident that a higher air hold-up produces a higher flotation yield. To enhance bitumen flotation recovery in practice, methyl isobutyl carbinol (MIBC) as a frother is added intentionally in some operations. One role of MIBC, known in mineral flotation practice, is to generate a sufficient amount of small and stable bubbles to carry desired solids to the slurry surface of flotation vessel. The froth layer built-up with such bubbles is sufficiently stable to maintain a certain depth (referred to as froth height), not only for reducing the need for tight control of slurry surface level, but also for facilitating the transfer of floated solids from the vessel to the collecting launder and minimizing water recovery and enhancing rejection of entrained solids.

It is well established that Athabasca bitumen contains various natural surfactants. Two major types of surfactants found in the bitumen process water are carboxylates and sulphonates, both containing oxygen functional groups (Moschopedis, Fryer et al., 1977; Ali, 1978; Schramm and Smith, 1987). These surface-active species adsorb at the air-water interface, reducing the surface tension and thus stabilizing air bubbles. In bitumen extraction, caustic is added to facilitate bitumen liberation from oil sand grains by ionizing natural surfactants in the bitumen (Isaacs and Smolek, 1983). However, Dai, Chung et al., 1992 found that an extremely fine white precipitate containing mostly calcium carbonate was produced by reacting bitumen with aqueous sodium hydroxide solution heated above 50°C. It is anticipated that the co-precipitation of divalent cations in the process water heated above 50°C can reduce the concentration of natural surfactants, resulting in the formation of less stable air bubbles. In our recent study, in fact, this temperature sensitivity showed a detrimental effect on bitumen flotation from a middling stream in an in-plant test with a flotation column.

The conventional CHWE process operates at temperatures approaching 75°C in order to lower the viscosity of bitumen to facilitate bitumen liberation and handling. This process is energy-intensive due to the necessity of heating large quantities of water to such high temperatures. Consequently, the oil sands industries have been focussing on the development of lower-energy extraction alternatives. Syncrude Canada Ltd. is the first to move to Low Energy Extraction process, operating at temperatures close to 35 °C. In this process, the lower thermal energy is made up through the addition of process aids such as kerosene and/or MIBC, but a fundamental understanding of the mechanisms involved remains to be explored. Although extensive research has been devoted to understanding the existing CHWE process, the results obtained could not be transferred to the development and commercialization of low-energy alternatives in industrial operations. The objective of this study is to gain an understanding of the effect of temperature on and the role of surfactants released from bitumen in the formation of sufficiently small and stable air bubbles required for high bitumen recovery. Since the formation of a froth head (referred to as froth height) is a measure of the stability of air bubbles, the bubble

stability was determined by measuring the froth height formed in a water column using recycle process water from a commercial oil sands extraction process. The bubble size was measured photographically.

4.2 Experimental

4.2.1 Materials and apparatus

Recycle process water, provided by Syncrude Canada Ltd. from its Aurora mine was used throughout the experimental study. Table 4.1 gives the properties of the recycle process water used for testing. Analytical grade NaOH and HCl from Fisher Scientific were used as pH modifiers. In this study, a glass column of 65 cm high and 3 cm in diameter as shown schematically in Figure 4.1 was constructed. The column was fitted with a 35 cm tall water jacket attached to a circulating water bath (Neslab RTE-111, Cole-Parmer, Canada). A sintered porous glass sparger was attached to the bottom of the column. In order to generate bubbles of different sizes, two spargers having different pore size distributions (10-20 and 20-40 microns respectively), were used. The air was supplied through a compressed air cylinder (extra-dry grade, Praxair) and was controlled to a desired flow rate via a rotameter (Matheson, Fisher Scientific). The images of bubbles generated were taken with a digital camera (Nikon Coolpix, Japan) and analysed using a computer program (Sigma Scan Pro 4).

Table 4.1 - Properties of the recycle process water used for testing

Property	Value
Surface Tension (mN/m)	64.9
pH	8.9
Oxidation/Reduction Potential (mV)	-81.4
Ca ²⁺ concentration (ppm)	49.1

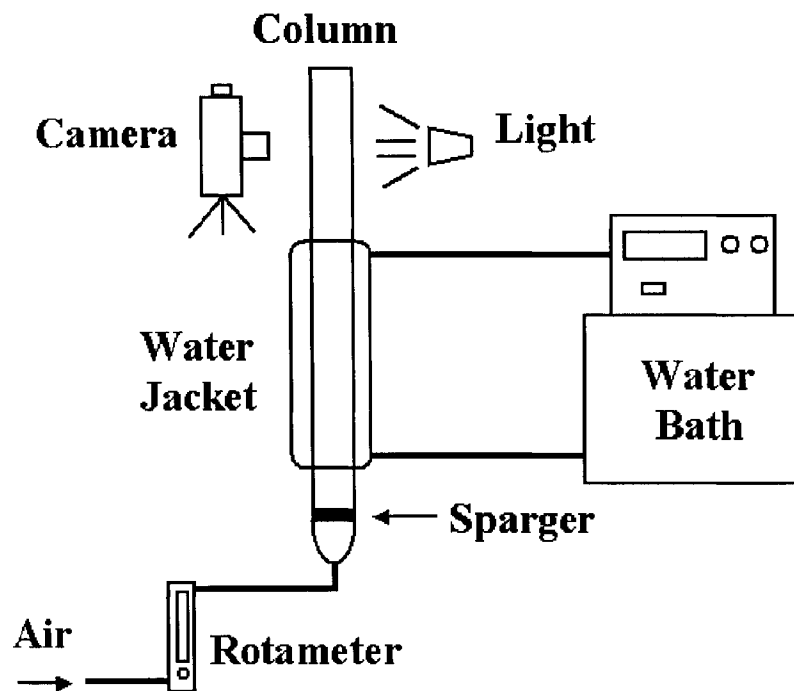


Figure 4.1 – Schematic illustration of experimental set-up

4.2.2 Experimental procedures

The recycle process water was first centrifuged at 2500 g using an ultracentrifuge (Beckman Allegro 64R) to remove fine solids. In each test, 250 mL of the centrifuged supernatant was placed in a volumetric flask, and immersed in the water bath at ambient temperature. The water bath was then set to a desired temperature ranging from 20 to 80°C. This ensured the solution to be heated or cooled gradually and precisely. The flask was taken out and shaken periodically to ensure thorough heating or cooling. Once the solution had reached the desired temperature, it was transferred into the column. The valve on the rotameter was then set to provide a desired airflow rate. Once a stable froth head was built (normally it took 90 seconds after the valve on the rotameter was opened), the height of the froth generated was recorded and reported in this communication, unless otherwise stated. A digital camera and bright backlight were used to record sharp images

of the bubbles in the bubbly region, just below the interface. These images were later analysed to determine the mean bubble diameter.

4.2.3 Experimental results

Figure 4.2 shows the result of froth height in the process water as a function of the water temperature, collected using fine and coarse spargers. The fine sparger has an average pore diameter of 15 microns, while the coarse sparger has an average pore diameter of 30 microns. The superficial air velocity was kept at 0.27 cm/s for the tests conducted with the fine sparger. When the coarse sparger was used, the superficial air velocity was increased to 0.67 cm/s in order to provide a sufficient upstream pressure behind the porous disk to generate bubbles evenly across the surface of the sparger. From this figure, it can be seen that the froth height decreases gradually with increasing recycle water temperature up to 60°C for the both cases. A further increase in recycle water temperature to 70°C causes the froth to collapse without formation of a visible froth layer. It is also observed that the height of froth produced with the coarser sparger is shorter than that formed with the finer sparger even though a higher gas rate was used in the coarser sparger case. This is attributed to the larger bubble size generated with the coarser sparger, as shown in Figure 4.3. Typical images of bubbles generated using the fine and coarse spargers are shown in Figure 4.4(a) and Figure 4.4(b), respectively.

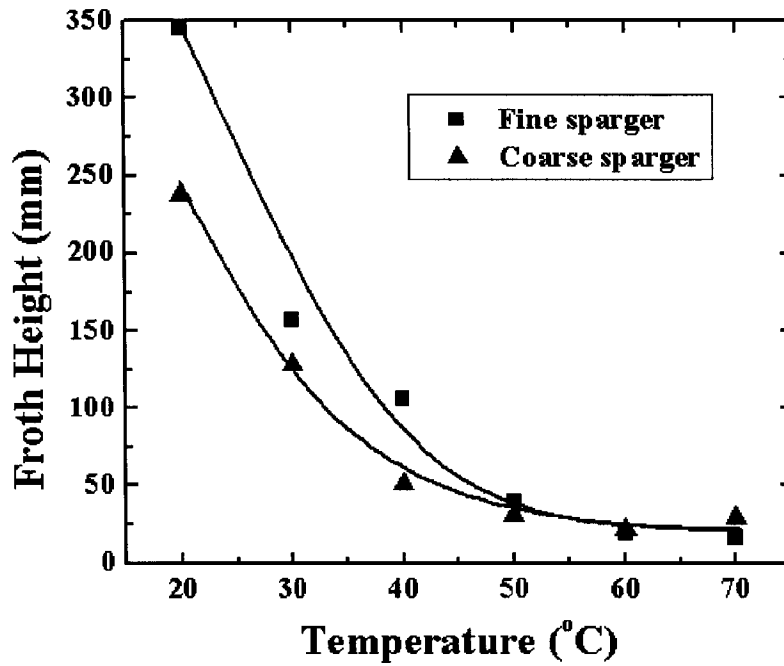


Figure 4.2 - Effect of recycle process water temperature on the froth height

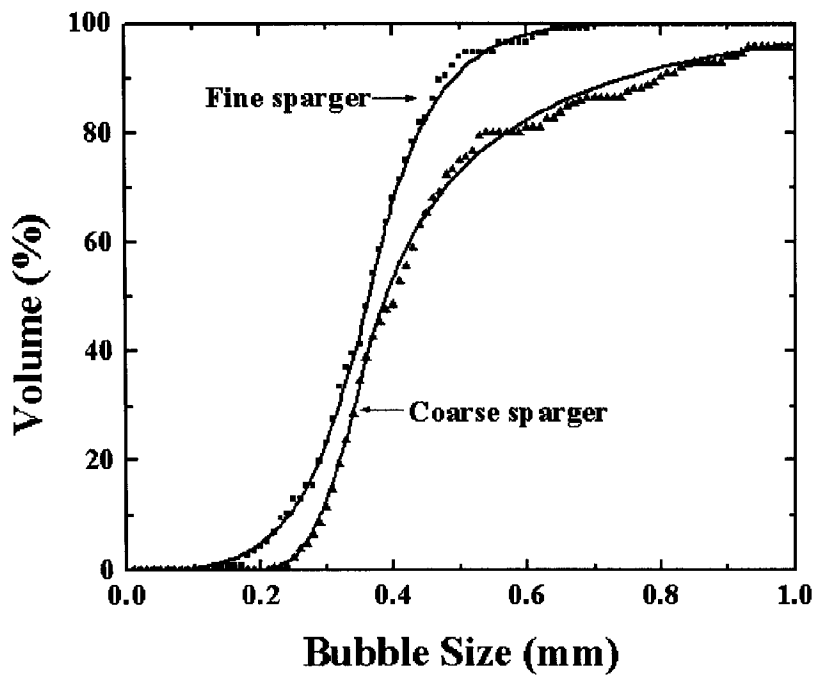


Figure 4.3 - Size distributions of bubbles generated using two different spargers

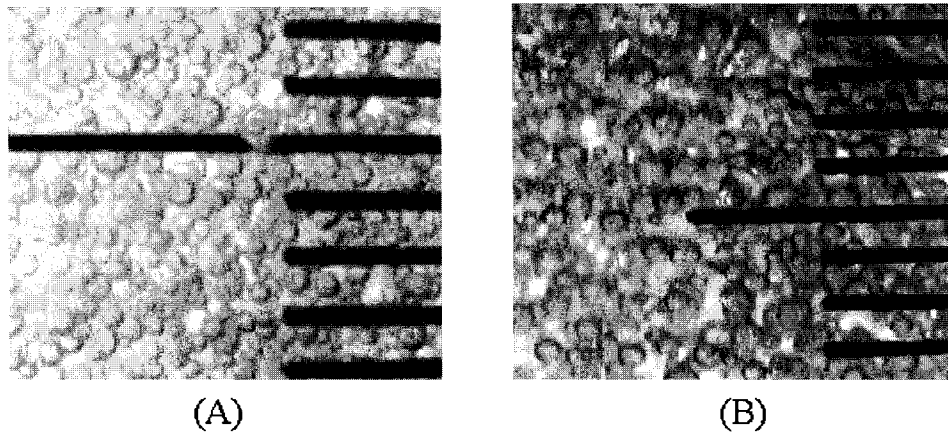


Figure 4.4 - Typical images of bubbles generated using (a) a fine and (b) a coarse sparger at 30°C; one small division = 1 mm

Figure 4.5 shows the change of froth height as a function of superficial air velocity in the recycle process water at different water temperatures. The tests were performed using the coarse sparger. As anticipated, the froth height increased with increasing airflow rate. The detrimental impact of temperature on bubble formation and stabilization was evident. At temperatures lower than 40°C, a linear increase in froth height with increasing the airflow rate was observed. Over the temperature range from 50 to 60°C, the froth formation appears to require a minimum superficial air velocity of about 0.7 cm/s, below which only a marginal froth layer was observed. It was observed that the bubbles formed over the minimum superficial air velocity are relatively large. They rise quickly and do not have sufficient time to build the froth before they collapse. At 70°C, the bubbles are unstable at all airflow rates tested. As a result, a froth layer is hardly observed, even at the highest superficial air velocity tested.

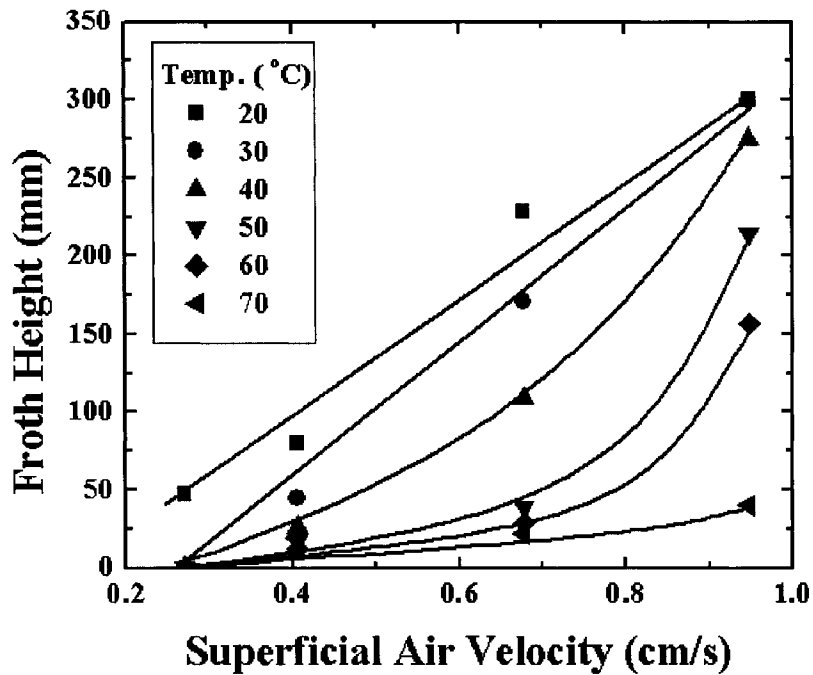


Figure 4.5 - Effect of recycle process water temperature on the froth height as a function of superficial air velocity

4.3 Discussion

To understand the observed froth height reduction with increasing recycle water temperature, the froth height and the mean size of the bubbles obtained under the same experimental conditions were plotted as a function of recycle water temperature. For illustrative purposes, the results collected with the coarse sparger at the superficial air velocity of 0.67 cm/s are shown in Figure 4.6. It is interesting to note that over the region where froth height reduced drastically with increasing the solution temperature to 50°C, there is little increase in bubble size. The significant increase in bubble size was observed to start at 60°C, at which froth height already reached minimal of 20 mm. This observation suggests that frothing and froth stability are not directly correlated to bubble size in the current study. It is important to mention that, during the tests, the formation of a precipitate was observed when the solution temperature exceeded 50°C. The precipitate was found to be insoluble even under mechanical agitation, but dissolved in an acid

solution at pH 2.5. It appears that bubble size increase may be related to the removal of surface-active species through precipitation.

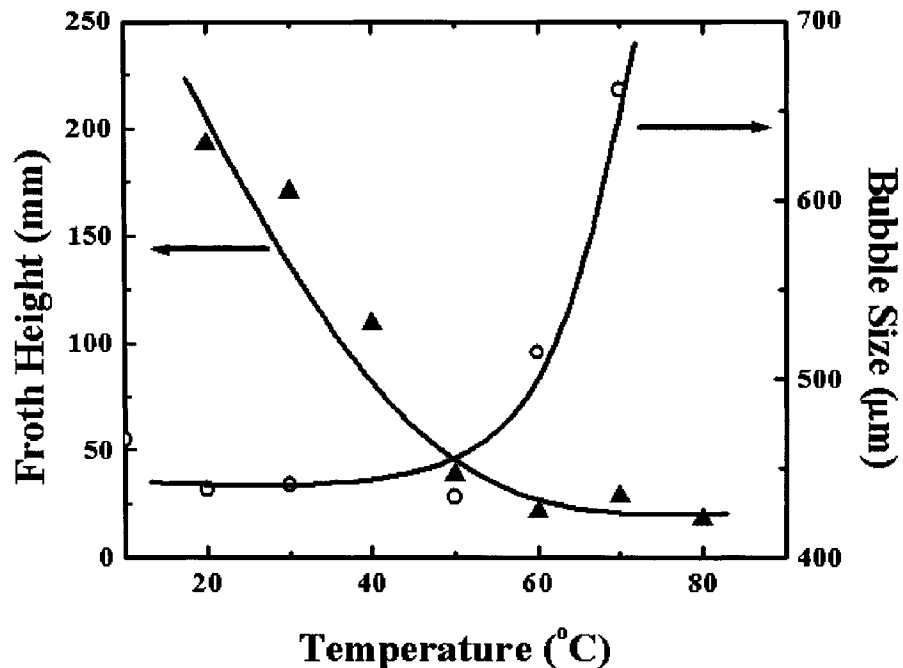


Figure 4.6 - Effect of recycle process water temperature on the froth height and the bubble size distribution

In order to study the effect of the precipitation on frothing and froth stability, the froth height was measured under various conditions. In one test, the recycle process water was gradually heated to 70°C in a beaker, during which a precipitate was observed to form. After the precipitate settled to the bottom of the beaker, the supernatant was carefully transferred to the column and a test was performed at 70°C and the same aeration conditions as used in the comparative tests with the as-received recycle process water. The froth height was reduced drastically after heating and removing the precipitate, as shown in Figure 4.7 (test 2). After the same solution was cooled down to 20°C, an improvement on the froth stability was observed with the froth height reaching 125 mm after prolonged aeration (Figure 4.7, test 3). To further test the role of chemical compounds forming the precipitate at high temperatures, another test was performed. In this test, the recycle process water was first heated up to 70°C to form the precipitate. The

precipitate-containing solution was then cooled to 20°C and the solution pH was lowered to 2.5 by adding diluted HCl solution. At this pH, the precipitate re-dissolved back into the recycle water. After complete dissolution of the precipitate, judged visually, the solution pH was raised back to the original value of 8.9 by adding dilute NaOH solution. With this reconstituted recycle water (labelled as 'control pH' in the figure), the froth height was found to be higher than that obtained at 20°C with the precipitate removed (Figure 4.7, test 4). However, a significant decrease in the froth height as compared with the initial recycle process water (test 1) was observed. From these results, it is reasonable to conclude that the decrease in froth stability, observed at water temperature above 50°C, was caused by changing water chemistry.

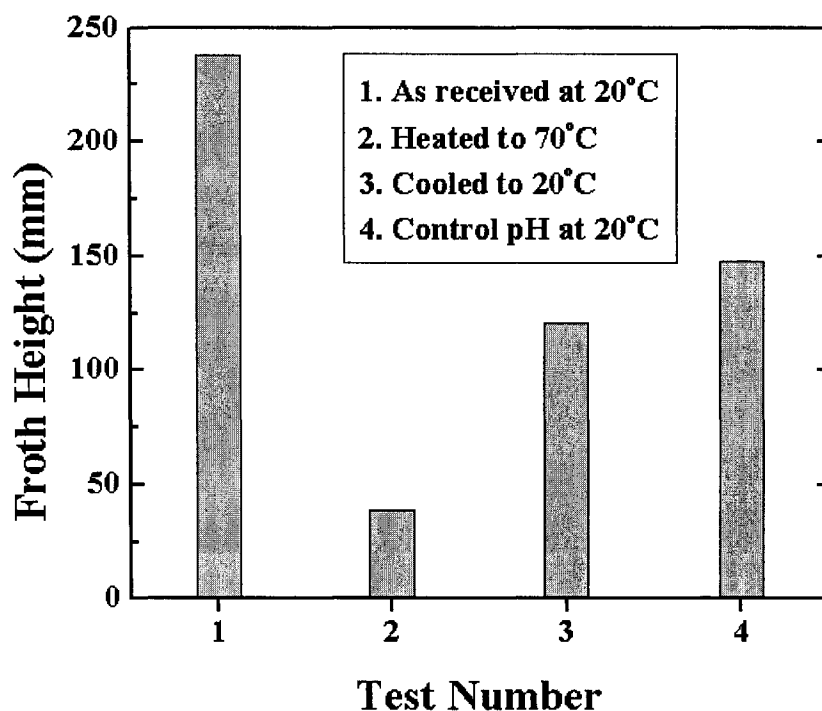


Figure 4.7 - Effect of precipitate on the froth height

There seem to be two parameters at work affecting froth stability. Comparison between tests 1 and 3 shows the effect of water chemistry where the precipitate was removed in test 3. Comparison between tests 2 and 3 shows the effect of temperature. One would expect tests 1 and 4 to give similar results for the froth height. However, there is some decrease in the froth stability for test 4 where the precipitate was re-dissolved. The

difference can be attributed to the loss of volatile surfactant compounds during the frothing tests in order to arrive at test 4.

To further understand the temperature effect, an attempt is made to characterize the precipitate formed in the recycle process water at temperatures close to 70°C. For this purpose, a given amount of the recycle process water was placed in a beaker and gradually heated to 70°C to allow the precipitate to form. The suspension was then cooled to room temperature and centrifuged to collect the precipitate. The precipitate was dried at 60°C under vacuum for 24 hours, and analyzed using an Energy Dispersive X-ray (EDX, Prism Intrinsic Germanium X-ray detector, Princeton Gamma-Tech) microanalysis. As shown in Figure 4.8, calcium represents the most abundant element in the precipitate, along with trace amounts of oxygen, sodium, magnesium, aluminium, silicon, sulphur, and chlorine. The Atomic Absorption (AA, Perkin Elmer 4000) analysis indicated that the precipitate contained about 33% calcium and 2% magnesium. The X-ray Diffraction (XRD, Philips 1710 with a Cu-K radiation) pattern does not indicate any evidence of the presence of crystalline calcium carbonate (e.g., calcite, aragonite, vaterite, etc.), as shown in Figure 4.9. The measured diffraction pattern is closely matched with a standard diffraction pattern of the acid fuchsin ($C_{20}H_{17}N_3O_9S_3Na_2$). Further analysis was conducted using a Fourier Transform Infrared Spectrometer (FTIR, FTS600, Bio-Rad Laboratories Inc) at its diffuse reflection mode (DRIFTS). Potassium bromide (KBr) was used as the background and characterization was performed at a 1:9 KBr to precipitate mass ratio. The FTIR results confirm the presence of various organic components. The major constituents in the precipitate were identified as carboxylates, sulphonates, amines and benzenes as indicated in Figure 4.10. This finding agrees with what was reported in the previous studies (Moschopedis, Fryer et al., 1977; Ali, 1978; Schramm and Smith, 1987). Therefore, from the EDX, XRD, and FTIR analyses, it is safe to conclude that the precipitate was not simply calcium carbonate, but rather than a complex mixture of organic and inorganic compounds. It was evident that the formation of a precipitate reduced the concentration of the ionized surfactants present in the recycle process water.

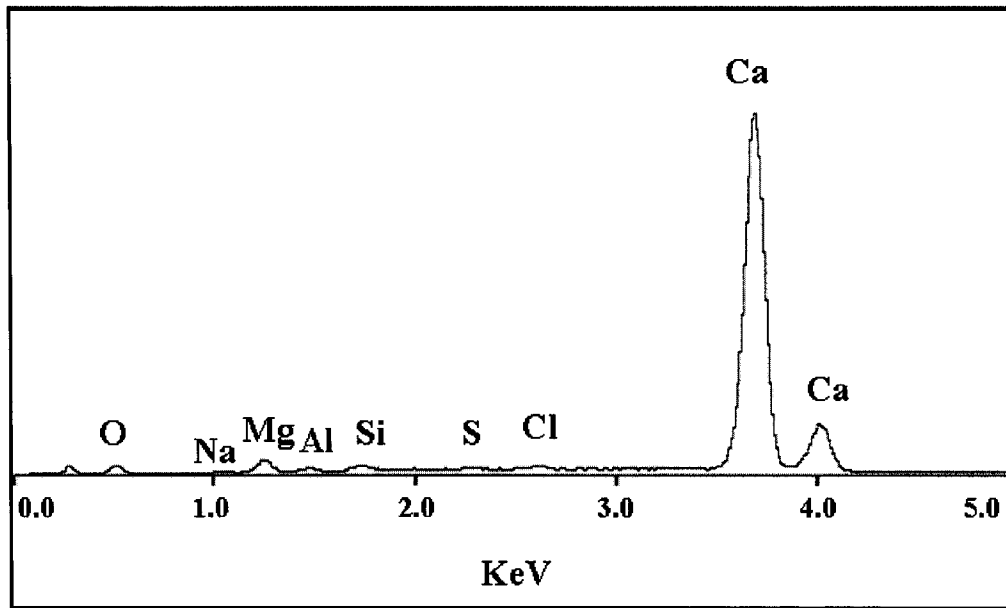


Figure 4.8 - EDX results obtained with the precipitate formed in recycle process water at 70°C.

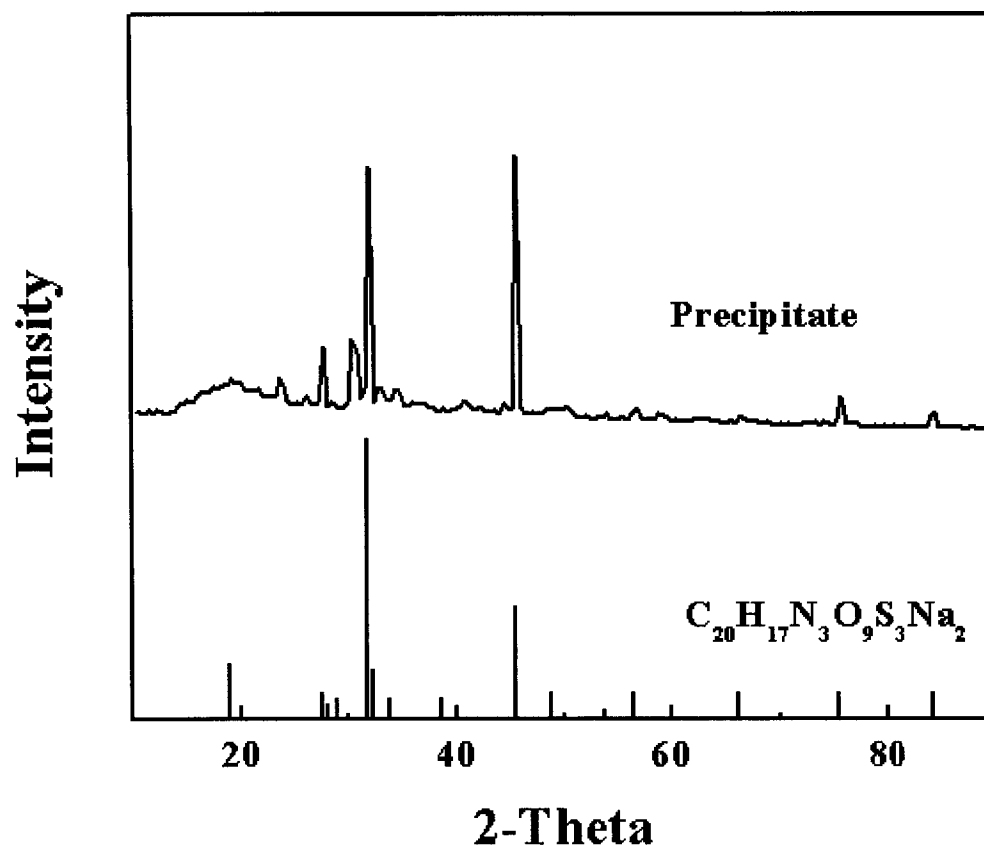


Figure 4.9 - XRD results obtained with the precipitate formed in recycle process water at 70°C.

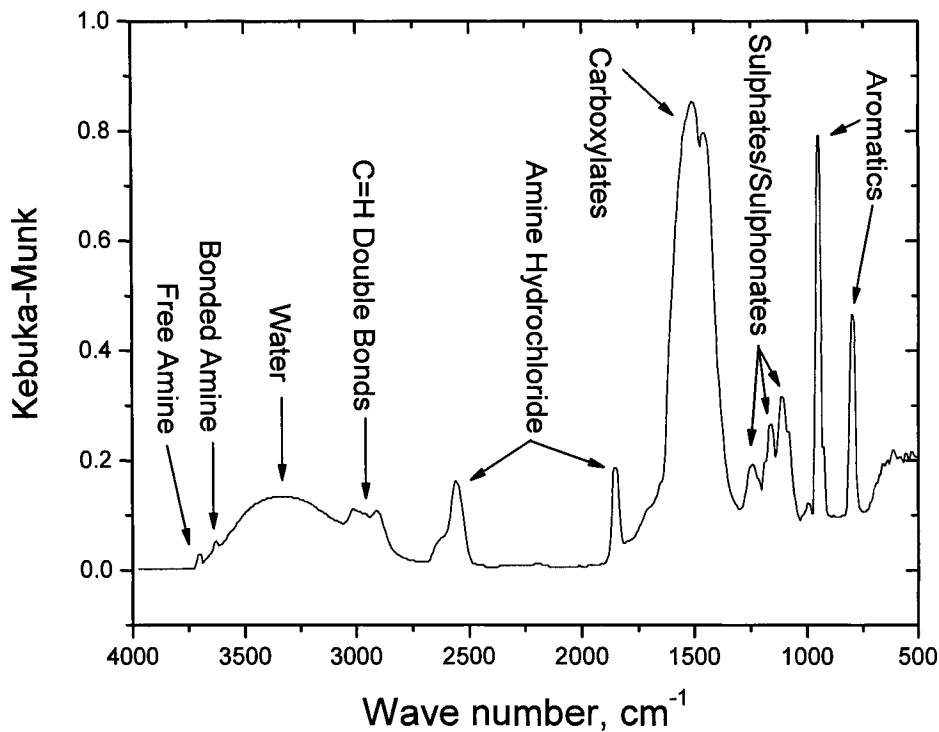


Figure 4.10 - FTIR results obtained with the precipitate formed in recycle process water at 70°C.

4.4 Conclusions

From this study, it can be concluded that heating the recycle process water removed some of the natural surfactants by precipitation. The depletion of these surfactants would lead to the need for higher NaOH dosage in the bitumen conditioning stage to generate sufficient amount of surfactants. High pH and high temperatures were identified to favour the precipitation. The main findings from this study can be summarized as follows:

- 1) Temperature played a major role in the stability of froth formed in oil sands extraction process water: the froth becomes less stable with increasing temperature.
- 2) Froth height increased with increasing airflow rate, but decreased with increasing temperature.

3) The formation of an insoluble precipitate was identified as the main cause for the reduction of froth stability with increasing process water temperature. Ionic natural surfactants including carboxylates, sulphonates and amines were removed from the process water by co-precipitation with calcium, resulting in a significantly negative impact on froth stability.

Chapter 5 – Summary and recommendations

In the present study, the recession of bitumen from a silica surface – either glass or quartz – was analysed under shear flow. Previous studies in the field had all observed the recession of bitumen from silica in a shear-free environment. It was desirable to determine how bitumen recession behaved under shear flow, as oil sands ore in the commercial operation is subjected to shearing flows of varying intensity as the oil sand slurry flows through pumps, pipelines, mechanical tumblers and/ or settling vessels.

Vacuum distillation unit feed bitumen, supplied by Syncrude Canada, Ltd., was diluted, centrifuged, and filtered to remove solids, then re-concentrated and used to coat microscope glass and quartz slides. These slides were subjected to a shearing flow of water in either a coaxial cylinder device, or a channel flow device. The rate at which the bitumen receded from the slide was measured using an optical technique.

Temperature and water chemistry were shown to have a significant influence on the recession rate of bitumen. In deionized water, the addition of divalent cations was shown to significantly impede the recession of bitumen from silica. Recession was found to improve slightly when the pH was increased. Recession was found to occur much faster at higher temperature in both deionized water and industrial recycle process water. Although the industrial process water contained significant amount of divalent cations, the recession rate in this water was only moderately slower than deionized water. The presence of natural surfactants and/or bicarbonates assisted in suppressing the effects of calcium and magnesium in the water. Moderate changes in the chemistry of the process water did not significantly affect the recession rate. It would appear that once a minimum concentration of surfactants and/or bicarbonates is reached, the levels of divalent cations and surface-active species no longer play a major role in bitumen recession.

It is recommended that bitumen extraction be performed in industrial recycle process water, and that the temperature of the slurry be maintained at or above 35°C. Recession

below this temperature is so slow that primary recovery is likely to be very poor without the addition of significant quantities of process aids or mechanical energy.

The velocity of water across the slide's surface was shown to have an effect on recession rate. Recession was observed to be faster at higher fluid flowrates. Therefore it is recommended that the shear stress be maintained at the highest practical value. While the abrasiveness of the oil sands slurry prevents the use of traditional static mixing elements or other methods of introducing shear, the slurry flowrate can simply be maintained at a high level in order to keep the slurry velocity high. In the case where extraction occurs in a mechanical tumbler; it is likely that increasing the tumbler's rotation speed will increase the rate of recession of bitumen.

Since the presence of natural surfactants and/or bicarbonates present in the oil sands recycle process water have been shown to enhance bitumen recession in the presence of divalent cations, it may be advisable for a newly started oil sands extraction operation to import a quantity of process water from another operation – especially if the raw water source contains significant concentrations of divalent ions. While the recycled process water would eventually absorb surfactants and other chemical species from the oil sands ore itself, it is likely that primary recovery would suffer until these species reached an appropriate level. It is recommended that further research be performed in this area. A pilot-scale test using a mixture of Athabasca river water and industrial recycle water would be especially useful in determining what the payback time for importing industrial process water would be.

Since the recession of bitumen from an oil sand ore sample *in situ* could not be successfully observed with the current experimental setup, it is recommended that another attempt to design an appropriate experimental apparatus for this application be made. Observation of bitumen recession *in situ* is the logical next step in the analysis of oil sands extraction work, as it applies to the ablation and liberation stage of the process.

Further study is also needed to determine which chemicals present in industrial process water are responsible for the enhancement of bitumen recession in the presence of divalent ions, and to determine the minimum concentrations required for effectiveness. Once that is determined, experiments where process water is doped with these chemicals can be made. Also, identification of these chemical species and concentrations would allow for better synthesis of process water for use when actual process water cannot be used (due to its contamination with fine clays, dissolved and emulsified oils, etc).

Bibliography:

- Ali, L. H. (1978). "Surface-Active Agents in the Aqueous Phase of the Hot-Water Flotation Process for Oil Sands." Fuel **57**(6): 357-360.
- Baptista, M. V. and C. W. Bowman (1969). The Flotation Mechanism of Solids from the Athabasca Oil Sand. 19th Canadian Chemical Engineering Conference, Edmonton, AB, Canada, Canadian Society for Chemical Engineering.
- Basu, S., K. Nandakumar, et al. (2004). "Effect of calcium ion and montmorillonite clay on bitumen displacement by water on a glass surface." Fuel **83**(1): 17-22.
- Basu, S., K. Nandakumar, et al. (1996). "A study of oil displacement on model surfaces." Journal of Colloid and Interface Science **182**(1): 82-94.
- Basu, S., K. Nandakumar, et al. (1998). "A visual study of high grade oil sand disintegration process." Journal of Colloid and Interface Science **205**(1): 201-203.
- Basu, S., K. Nandakumar, et al. (2000). "Study on daughter droplets formation in bitumen/glass/water contact line displacement due to instability." Fuel **79**(7): 837-841.
- Basu, S. and M. M. Sharma (1996). "Measurement of critical disjoining pressure for dewetting of solid surfaces." Journal of Colloid and Interface Science **181**(2): 443-455.
- Bird, R. B., W. E. Stewart, et al. (2002). Transport Phenomena. New York, USA, John Wiley & Sons, Inc.
- Choung, J., J. Walker, et al. (2004). "Effect of temperature on the stability of froth formed in the recycle process water of oil sands extraction." Canadian Journal of Chemical Engineering **82**(4): 801-806.
- Cox, R. G. (1986). "Dynamics of the Spreading of Liquids on a Solid Surface. Part 1. Viscous Flow." Journal of Fluid Mechanics **168**: 169-194.
- Dai, Q. and K. H. Chung (1995). "Bitumen--sand interaction in oil sand processing." Fuel **74**(12): 1858-1864.
- Dai, Q., K. H. Chung, et al. (1992). "Formation of Calcium Carbonate in the Bitumen/Aqueous Sodium Hydroxide System." AOSTRA Journal of Research **8**: 95-101.

- Foister, R. T. (1990). "Kinetics of displacement wetting in liquid/liquid/solid systems." Journal of Colloid and Interface Science **136**(1): 266-282.
- Fox, R. W., A. T. McDonald, et al. (2004). Introduction to Fluid Mechanics, John Wiley & Sons.
- Garaud, P. and G. I. Ogilvie (2005). "A model for the nonlinear dynamics of turbulent shear flows." Journal of Fluid Mechanics **530**: 145-176.
- Hepler, L. G. and R. G. Smith (1994). "The Alberta Oil Sands: Industrial Procedures for Extraction and some Recent Fundamental Research." AOSTRA Technical Publication Series **14**.
- Hunter, R. J. (1986). Foundations of Colloid Science, Volume 1. Oxford, Clarendon Press.
- Ignasiak, T. M., Q. Zhang, et al. (1985). "Chemical and Mineral Characterization of the Bitumen-Free Athabasca Oil Sands Related to the Bitumen Concentration in the Sand Tailings from the Syncrude Batch Extraction Test." AOSTRA Journal of Research **2**: 21-35.
- Isaacs, E. E. and K. F. Smolek (1983). "Interfacial Tension Behavior of Athabasca Bitumen/Aqueous Surfactant Systems." Canadian Journal of Chemical Engineering **61**(2): 233-240.
- Jacobs, F. A., J. K. Donnelly, et al. (1980). "Viscosity of Gas-Saturated Bitumen." Journal of Canadian Petroleum Technology **19**(4): 46-50.
- Kotlyar, L. S. and B. D. Sparks (1985). "Isolation of Inorganic Matter-Humic Complexes from Athabasca Oil Sands." AOSTRA Journal of Research **2**: 103-111.
- Liu, J., Z. Xu, et al. (2003). "Studies on bitumen-silica interaction in aqueous solutions by atomic force microscopy." Langmuir **19**(9): 3911-3920.
- Liu, J., Z. Zhou, et al. (2002). "Bitumen-clay interactions in aqueous media studied by zeta potential distribution measurement." Journal of Colloid and Interface Science **252**(2): 409-418.
- Masliyah, J., Z. Zhou, et al. (2004). "Understanding water-based bitumen extraction from athabasca oil sands." Canadian Journal of Chemical Engineering **82**(4): 628-654.

- McIntyre, D. D., D. S. Montgomery, et al. (1985). "Carboxylic Acids Bound to the Mineral Matter in Heavy Cretaceous Oils of Alberta." AOSTRA Journal of Research **2**: 223-231.
- Moschopedis, S. E., J. F. Fryer, et al. (1977). "Water-soluble constituents of Athabasca bitumen." Fuel **56**(1): 109-110.
- Moschopedis, S. E. and J. G. Speight (1971). "Water-soluble derivatives of Athabasca asphaltenes." Fuel **50**(1): 34-40.
- Radler, M. (2002). "Worldwide reserves increase as production holds steady." Oil & Gas Journal **100**(52): 113.
- Redon, C., F. Brochard-Wyart, et al. (1991). "Dynamics of dewetting." Physical Review Letters **66**(6): 715-718.
- Resources, A. C. o. (2004). "Oil Sands Technology Roadmap – Unlocking the Potential." Retrieved May 9, 2006.
- Sanford, E. C. and F. A. Seyer (1979). "PROCESSIBILITY OF ATHABASCA TAR SAND USING A BATCH EXTRACTION UNIT: THE ROLE OF NaOH." CIM Bull **72**(803): 164-169.
- Schlichting, H. (1979). Boundary-Layer Theory, McGraw-Hill Book Company.
- Schramm, L. L. and R. G. Smith (1987). "Two Classes of Anionic Surfactants and Their Significance in Hot Water Processing of Oil Sands." Canadian Journal of Chemical Engineering **65**(5): 799-811.
- Schramm, L. L., R. G. Smith, et al. (1984). "Surface-Tension Method for the Determination of Anionic Surfactants in Hot Water Processing of Athabasca Oil Sands." Colloids and Surfaces **11**(3-4): 247-263.
- Schramm, L. L., E. N. Stasiuk, et al. (2003). "Temperature effects from the conditioning and flotation of bitumen from oil sands in terms of oil recovery and physical properties." Journal of Canadian Petroleum Technology **42**(8): 55-61.
- Shull, K. R. and T. E. Karis (1994). "Dewetting dynamics for large equilibrium contact angles." Langmuir **10**(1): 334-339.
- Srinivasan, N. S. (1989). Review of Studies on Bitumen. Edmonton, AB, Canada, Syncrude Canada Ltd. Research Department.

Syncrude Canada, L. (2006). "What We Do at Syncrude." Retrieved May 9, 2006, from http://www.syncrude.ca/who_we_are/01_04.html.

Wallwork, V., Z. Xu, et al. (2004). "Processibility of athabasca oil sand using a Laboratory Hydrotransport Extraction System (LHES)." Canadian Journal of Chemical Engineering **82**(4): 687-695.

Zhou, Z., Z. Xu, et al. (2000). "Effect of natural surfactants released from Athabasca oil sands on air holdup in a water column." Canadian Journal of Chemical Engineering **78**(4): 617-624.